Matrix elements of ΔB=0 operators in heavy hadron chiral perturbation theory

Jong-Wan Lee

Phys. Rev. D **91**, 094511 — Published 26 May 2015

DOI: 10.1103/PhysRevD.91.094511

Matrix elements of $\Delta B = 0$ operators in heavy hadron chiral perturbation theory

Jong-Wan Lee*

Department of Physics, The City College of New York, New York, NY 10031, USA

Abstract

We study the light-quark mass and spatial volume dependence of the matrix elements of $\Delta B = 0$ four-quark operators relevant for the determination of V_{ub} and the lifetime ratios of single-b hadrons. To this end, one-loop diagrams are computed in the framework of heavy hadron chiral perturbation theory with partially quenched formalism for three light-quark flavors in the isospin limit; flavor-connected and -disconnected diagrams are carefully analyzed. These calculations include the leading light-quark flavor and heavy-quark spin symmetry breaking effects in the heavy hadron spectrum. Our results can be used in the chiral extrapolation of lattice calculations of the matrix elements to the physical light-quark masses and to infinite volume. To provide insight on such chiral extrapolation, we evaluate the one-loop contributions to the matrix elements containing external B_d, B_s mesons and Λ_b baryon in the QCD limit, where sea and valence quark masses become equal. In particular, we find that the matrix elements of the λ_3 flavor-octet operators with external B_d meson receive the contributions solely from connected diagrams in which current lattice techniques are capable of precise determination of the matrix elements. Finite volume effects are at most a few percent for typical lattice sizes and pion masses.

PACS numbers: 12.38Gc,12.39Fe,12.39Hg,14.20.Mr,14.40.Nd

*Electronic address: jwlee2@ccny.cuny.edu

I. INTRODUCTION

In inclusive decays of single-b hadrons, the effects of spectator quarks (light constituent quarks in the hadrons) play an important role in extracting their decay widths and the lifetimes of different species as those quarks participate in the weak process. In particular, for a number of years there have been suggestions that the lifetime of the Λ_b baryon had significant corrections from the spectator effects [1, 2], which might explain the small experimental value of the lifetime ratio $\tau(\Lambda_b)/\tau(B_d)$. Recent measurements tend to favor more natural values [3] :

$$\frac{\tau(B^+)}{\tau(B_d)} = 1.079 \pm 0.007, \qquad \frac{\tau(B_s)}{\tau(B_d)} = 0.993 \pm 0.009, \qquad \frac{\tau(\Lambda_b)}{\tau(B_d)} = 0.930 \pm 0.020. \tag{1}$$

Theoretical determinations of these lifetime ratios rely on the heavy quark expansion (HQE) for inclusive decays with one heavy quark in the final state [4–7]. Although the Λ_b lifetime is no longer a puzzle, it is desired to improve the theoretical determinations of the lifetime ratios since their uncertainties are larger than those of experimental measurements by an order of magnitude except $\tau(B_s)/\tau(B_d)$ [8]. In particular, the dominant source of systematic uncertainties in the HQE predictions are the size of the non-perturbative matrix elements of the dimension-six $\Delta B = 0$[1] four-quark operators containing spectator quarks, which are poorly known from exploratory lattice studies [9–11] and QCD sum rules [12–15]. Thus, the determination of these matrix elements from the state-of-the-art lattice calculations will significantly reduce the uncertainties and play an essential role in the precision test of the HQE.[2]

The theoretical calculation of the decay width can be done systematically using the optical theorem, which relates the total decay rate of the single-b hadron H_b to the imaginary part of the matrix element of the forward scattering amplitude,

$$\Gamma(H_b \to X) = \frac{1}{M_{H_b}} \mathrm{Im} \langle H_b | \mathbf{T} | H_b \rangle, \tag{2}$$

[1] ΔB denotes the change of b-quark number by the operators.

[2] As emphasized in a recent review paper about the current status of the HQE [16], the HQE is now in the era of precision tests as the significant discrephancies between the HQE predictions and experimental measurements are resolved for the Λ_b lifetime and the semileptonic branching ratios of B mesons. Moreover, the validity of the HQE is strongly supported from the fact that the recent measurement of the decay rate differences $\Delta\Gamma_s$ [3] perfectly agrees with the HQE predictions [17].

where M_{H_b} is the hadron mass. Here the transition operator $\mathbf{T}$ is given by

$$\mathbf{T} = i \int d^4x T\{\mathcal{L}_{eff}(x), \mathcal{L}_{eff}(0)\}, \tag{3}$$

where $\mathcal{L}_{eff}$ represents the effective $\Delta B = 1$ weak Lagrangian renormalized at the scale of b-quark mass, $\mu = m_b$. Since the energy release is large ($\sim m_b$) in b-hadron decays, the operator product expansion (OPE) is applicable to construct local $\Delta B = 0$ operators having the same quantum numbers, with suppression by inverse powers of m_b accompanying increasing operator dimensions.[3] Using the OPE, one can write the decay width by

$$\Gamma(H_b \to X) = \frac{G_F^2 m_b^5}{192\pi^3} \frac{1}{2M_{H_b}} \sum_k \frac{c_k(\mu)}{m_b^{k-3}} \langle H_b | \mathcal{O}_k^{\Delta B=0} | H_b \rangle, \tag{4}$$

where $c_k(\mu)$ and $\mathcal{O}_k^{\Delta B=0}$ represent Wilson coefficients containing relevant CKM matrix elements and dimension-k $\Delta B = 0$ local operators, respectively. The forward matrix elements of the local operators in Eq. 4 are systematically expanded with inverse power of m_b in the framework of heavy quark effective theory (HQET) [23–25]. This is the basic structure of the HQE. In these expansions the leading-order term is universal for all kinds of b hadrons. It is well known that deviations of the lifetime ratios first arise from the terms of order $1/m_b^2$ which include the nonperturbative corrections to $\langle H_b | \bar{b} b | H_b \rangle$ in the HQET and the subleading terms in the OPE, $\bar{b} g_s i \sigma_{\mu\nu} G^{\mu\nu} b$, whose dimension is five [5–7]. The spectator effects contribute to the process at the order of $1/m_b^3$, where the corresponding dimension-six

[3] It is well known that the OPE breaks down when one calculates differential inclusive B-meson decay distributions near the endpoint region in phase space, where a proper treatment of forward matrix elements of non-local operators is required [18–20]. Although the non-local operators typically reduce to local ones if the decay distributions are integrated over all phase space, there are cases such as the inclusive radiative decay $B \to X_s\gamma$ in which certain non-local matrix elements have sizable corrections to the total decay rate [21, 22]. However, we note that in the case of the total inclusive decay rates of single-b hadrons (i.e. all final states are summed), which is relevant for the determination of lifetimes, it is believed that the standard OPE is applicable.

$\Delta B = 0$ four-quark operators in a convenient basis are given by [1][4]

$$\begin{aligned}
\mathcal{O}_{1,a} &= \bar{b}^\alpha \gamma_\mu (1-\gamma_5) q^{a,\alpha} \bar{q}_a^\beta \gamma^\mu (1-\gamma_5) b^\beta, \\
\mathcal{O}_{2,a} &= \bar{b}^\alpha (1-\gamma_5) q^{a,\alpha} \bar{q}_a^\beta (1+\gamma_5) b^\beta, \\
\mathcal{O}_{3,a} &= \bar{b}^\alpha \gamma_\mu (1-\gamma_5) q^{a,\beta} \bar{q}_a^\alpha \gamma^\mu (1-\gamma_5) b^\beta, \\
\mathcal{O}_{4,a} &= \bar{b}^\alpha (1-\gamma_5) q^{a,\beta} \bar{q}_a^\alpha (1+\gamma_5) b^\beta,
\end{aligned} \tag{5}$$

where b denotes a b-quark field and q^a denotes a light-quark field of flavor a. The color indices α, β and the Lorentz indices μ are summed, but the flavor indices a are not. In fact, although these effects are suppressed by an additional power of $1/m_b$, the contributions are numerically enhanced by a phase-space factor of $16\pi^2$ [1].

It was also pointed out that the contribution of the four-quark operators in Eq. 5 can be significant to the inclusive decay $B \to X_u \ell \nu_\ell$ which is closely related to the determination of V_{ub} [26]. The four-quark operators relevant to this semi-leptonic decay are given by $\mathcal{O}_{1,u} - \mathcal{O}_{2,u}$ at the scale $\mu = m_b$ and their matrix elements can be parameterized by

$$\frac{1}{M_B}(\langle B|\mathcal{O}_{1,u}|B\rangle - \langle B|\mathcal{O}_{2,u}|B\rangle) = f_B^2 M_B (B_1 - B_2), \tag{6}$$

where f_B and M_B are the decay constant and the mass of B meson, respectively, and B_1 and B_2 are phenomenological parameters called bag constants. In the vacuum insertion approximation (or factorization) [27, 28], we have $B_1 = B_2$ and the spectator effects in Eq. 6 vanish. However, the actual values of these matrix elements should be determined from non-perturbative calculations and can be much different than that from the factorization approximation. In Ref. [26], for instance, the author showed that the correction to the branching ratio, $\delta B(B \to X_u \ell \nu_\ell)$, by spectator effects substantially enhances the estimate of the corresponding errors in the hybrid expansion, e.g. a violation of the relation $B_1 = B_2$ by 10% makes the correction of the branching ratio twice larger than the estimated uncertainty in Ref. [29].

In the OPE, the Wilson coefficients $c_k(\mu)$, which embed the dependence on scale μ, are determined from perturbative calculations while the matrix elements of local four-quark

[4] For $s_\ell = 0$ single-b baryons, only the first two four-quark operators are sufficient to compute the spectator effects in the heavy-quark limit, because $\mathcal{O}_1$ ($\mathcal{O}_2$) are related to $\mathcal{O}_3$ ($\mathcal{O}_4$) up to $1/m_b$ corrections via a Fierz transformation thanks to heavy-quark symmetry.

operators can be computed nonpertubatively, potentially from lattice QCD (see Ref. [16] and references therein). From the point of view of lattice QCD, difficulties arise from the fact that the light quark q in the operators can be different from the light valence-quark q' in the single-b hadrons, i.e. q's are contracted to themselves, so called eye-contractions [26]: the operators could mix with lower dimensional ones requiring a power-law subtraction. In addition, lattice calculations of the matrix elements including disconnected diagrams generally suffer from a noise problem. Although it is inevitable to avoid such difficulties in the calculation of the semi-leptonic decay, it is expected that the contributions of the eye-contractions are negligible in the calculation of the B-meson lifetime ratios due to the light-quark flavor symmetry. In particular, we find that the matrix elements of the λ_3 flavor-octet operators involving external B_d meson, which are relevant to the determination of $\tau(B^+)/\tau(B_d)$, do not only exclude the eye-contractions, but also the disconnected contributions[5] at the next-to-leading order in chiral expansion.

The purpose of this paper is to compute the one-loop chiral corrections, which are functions of light-quark mass (or pion mass), to the matrix elements of $\Delta B = 0$ four-quark operators in Eq. 5. At present, the light-quark masses in many lattice studies are not physical due to limited computing resources, and thus the chiral extrapolation to the physical quark masses is essential to obtain the matrix elements with high-precision. To do this, we consider heavy hadron chiral perturbation theory (HHχPT) [30–34] at finite volume [35–37] as the machinery to write the four-quark operators in terms of low-energy degrees of freedom, heavy hadrons and Goldstone mesons. Moreover, our calculation is performed in partially quenched chiral perturbation theory (PQχPT) [38] which is appropriate for current and foreseeable lattice calculations, as well as it naturally distinguishes disconnected diagrams from connected ones. Although the heavy quarks are assumed to be static, we consider the leading effect of various mass differences among B mesons and single-b baryons. For B mesons, the chiral corrections to the matrix elements of infinite volume QCD were previously calculated in Ref. [39].

The organization of this paper is as follows. In Sec. II, we briefly review heavy hadron chiral perturbation theory involving hadrons containing a single-b quark in SU(6|3) partially

[5] More precisely, the "disconnected" means the flavor-disconnected in which the light-flavor quarks in the operators are not connected with those in the external hadrons. Throughout this paper, similarly, the "singlet" and "octet" mean the flavor-singlet and -octet, respectively.

quenched theories. Mass differences in the heavy hadron spectrum, which originate from the light-quark flavor and heavy-quark spin symmetry breakings, are discussed in detail, where the relevant mass parameters enter the one-loop chiral computations. Sec. III contains the determination of $\Delta B = 0$ four-quark operators in partially quenched heavy hadron chiral perturbation theory. In Sec. IV, we present our main results: calculation of the matrix elements of the four-quark operators including one-loop chiral contributions at infinite volume and in a finite spatial box, where connected and disconnected contributions are clearly separated. Integrals and sums appearing in the loop calculations are summarized in Appendix A, while coefficients for these calculations involving B mesons and single-b baryons are summarized in Appendices B and C, respectively. Moreover, the pion-mass dependence of chiral corrections and finite volume effects are discussed for the exemplified cases of external B_d, B_s mesons and Λ_b baryon. Finally, we conclude our work in Sec. V.

II. PARTIALLY QUENCHED HEAVY HADRON CHIRAL PERTURBATION THEORY

The interactions of heavy hadrons containing a heavy quark with Goldstone mesons can be described in the framework of chiral perturbation theory (χPT) combined with the HQET. The inclusion of the heavy-light mesons into χPT was first carried out in [30–32] and extended to quenched and partially quenched theories in [40, 41]. The $1/M_P$ and chiral corrections were investigated in [42], where M_P is the mass of the heavy-light pseudo-scalar meson. The superfield appearing in this effective theory is [43]

$$H_i^{(\bar{b})} \;=\; \left(P_{i,\mu}^{*(\bar{b})}\gamma^\mu - P_i^{(\bar{b})}\gamma_5\right)\frac{1-\not{v}}{2}, \tag{7}$$

where $P_i^{(\bar{b})}$ and $P_{i,\mu}^{*(\bar{b})}$ annihilate pseudo-scalar and vector mesons containing an anti-b quark and a light quark of flavor i. For convenience, the space-time variables in the fields and transformations do not explicitly appear throughout this paper (e.g. $H_i^{(\bar{b})}(x) = H_i^{(\bar{b})}$). In the heavy quark formalism, the momentum of such mesons is given as $p^\mu = M_P v^\mu + k^\mu$ with $k^\mu \ll M_P$, where v^μ is the 4-velocity of the meson fields. Under a heavy quark spin SU(2) transformation S_h and a light-flavor transformation U [i.e., $U \in$ SU(3) for full QCD and $U \in$ SU(6|3) for partially quenched QCD (PQQCD)], the field $H^{(\bar{b})}$ transforms as

$$H_i^{(\bar{b})} \to U_i{}^j H_j^{(\bar{b})} S_h^{-1}.$$

The conjugate field, which creates mesons containing an anti-b quark and a light quark of flavor i, is defined as

$$\bar{H}_i^{(\bar{b})} = \gamma^0 H_i^{(\bar{b})\dagger}\gamma_0 = \frac{1-\not{v}}{2}\left(P_{i,\mu}^{*(\bar{b})\dagger}\gamma^\mu + P_i^{(\bar{b})\dagger}\gamma_5\right), \tag{8}$$

and transforms under S_h and U as

$$\bar{H}_i^{(\bar{b})} \to S_h \bar{H}_j^{(\bar{b})} U^{\dagger j}{}_i. \tag{9}$$

The inclusion of baryons containing a b-quark and two light quarks into χPT was first proposed in [32–34], and the effective theory was generalized to the quenched and partially quenched theories in [44–46]. In the limit $m_b \to \infty$, the heavy quark's spin decouples from the system and the total spin of the light degrees of freedom is conserved. Because of this property of the heavy-quark symmetry, one can classify baryons by the total spin quantum number of the light degrees of freedom, $s_\ell = 0$ or $s_\ell = 1$. These two types of baryons carrying light flavors i and j can be included into SU(6|3) PQχPT by introducing the corresponding interpolating fields at the quark level as

$$\begin{aligned}
\mathcal{T}_{ij}^{\gamma} &\sim b^{\gamma,c}\left(q_i^{\alpha,a}q_j^{\beta,b} + q_i^{\beta,b}q_j^{\alpha,a}\right)\epsilon_{abc}(C\gamma_5)_{\alpha\beta} \text{ for } s_\ell = 0, \\
\mathcal{S}_{ij}^{\gamma} &\sim b^{\gamma,c}\left(q_i^{\alpha,a}q_j^{\beta,b} - q_i^{\beta,b}q_j^{\alpha,a}\right)\epsilon_{abc}(C\gamma^\mu)_{\alpha\beta} \text{ for } s_\ell = 1,
\end{aligned} \tag{10}$$

where C is the charge-conjugation matrix, α, β, γ are the Dirac indices, and a, b, c are color indices. These flavor tensor interpolating fields satisfy

$$\mathcal{T}_{ij} = (-)^{\eta_i\eta_j}\mathcal{T}_{ji}, \quad \mathcal{S}_{ij}^{\mu} = (-1)^{1+\eta_i\eta_j}\mathcal{S}_{ji}^{\mu}, \tag{11}$$

where the grading factor η_k accounts for different statistics of quarks in PQQCD,

$$\eta_i = \begin{cases} 1 \text{ for } k = 1,2,3,4,5,6 \text{ (valence and sea)}, \\ 0 \text{ for } k = 7,8,9 \text{ (ghost)}. \end{cases} \tag{12}$$

The $\mathcal{T}$ and $\mathcal{S}$ fields form a **39**- and a **42**-dimensional representations of SU(6|3), respectively. The baryon fields appearing in HHχPT have the same flavor properties of the corresponding interpolating fields as in Eq. 11, where the combination of the heavy-quark spin 1/2 and the total spin of light quarks s_ℓ leads us that T baryon carries spin 1/2, while S baryon carries both spin 1/2 and 3/2 which are degenerate in the heavy-quark limit. If we restrict our attention to the pure valence-valence sector, we recover the familiar baryon tensors of

QCD. For $s_\ell = 0$, the baryon tensor $T_{ij}^{(\text{valence-valence})}$ is anti-symmetric under the exchange of light-quark flavor indices and explicitly written as

$$T_{ij}^{(\text{valence-valence})} = \frac{1}{\sqrt{2}} \begin{pmatrix} 0 & \Lambda_b & \Xi_b^{+1/2} \\ -\Lambda_b & 0 & \Xi_b^{-1/2} \\ -\Xi_b^{+1/2} & -\Xi_b^{-1/2} & 0 \end{pmatrix}, \tag{13}$$

where the superscript indicates the 3-component of the isospin. For $s_\ell = 1$, the baryon tensor S_{ij} is described by the superfield

$$S_\mu^{ij} = \sqrt{\frac{1}{3}}(\gamma_\mu + v_\mu)\gamma^5 B^{ij} + B_\mu^{*ij}, \tag{14}$$

where B_{ij} and $B_{ij}^{*\mu}$ are spin-1/2 and 3/2 baryons, respectively.[6] In the valence-valence sector, the baryon tensor $B_{ij}^{(\text{valence-valence})}$ is symmetric under the exchange of light-quark flavor indices and explicitly written as

$$B_{ij}^{(\text{valence-valence})} = \begin{pmatrix} \Sigma_b^{+1} & \frac{1}{\sqrt{2}}\Sigma_b^0 & \frac{1}{\sqrt{2}}\Xi_b^{\prime+1/2} \\ \frac{1}{\sqrt{2}}\Sigma_b^0 & \Sigma_b^{-1} & \frac{1}{\sqrt{2}}\Xi_b^{\prime-1/2} \\ \frac{1}{\sqrt{2}}\Xi_b^{\prime+1/2} & \frac{1}{\sqrt{2}}\Xi_b^{\prime-1/2} & \Omega_b \end{pmatrix}, \tag{15}$$

and similarly for the $B_{ij}^{*\mu}$ fields. Under the heavy-quark spin transformation S_h and the light-flavor transformation U,

$$\begin{aligned} T_{ij} &\longrightarrow S_h U_i{}^k U_j{}^\ell T_{k\ell}, \\ S_{ij}^\mu &\longrightarrow S_h U_i{}^k U_j{}^\ell S_{k\ell}^\mu. \end{aligned} \tag{16}$$

The conjugate fields, which create single-b baryons, are denoted as $\bar{S}_{ij}^\mu$ and $\bar{T}_{ij}$.

In PQχPT, the leading-order (LO) chiral Lagrangian for the Goldstone mesons is

$$\mathcal{L} = \frac{f^2}{8}\text{str}[(\partial^\mu \Sigma^\dagger)(\partial_\mu \Sigma) + 2B_0(\Sigma^\dagger \mathcal{M}_q + \mathcal{M}_q^\dagger \Sigma)] + \alpha_\Phi (\partial^\mu \Phi_0)(\partial_\mu \Phi_0) - M_0^2 \Phi_0^2, \tag{17}$$

where $\Sigma = \exp(2i\Phi/f) = \xi^2$ is the nonlinear Goldstone field, with Φ being the matrix containing the standard Goldstone fields in the quark-flavor basis. In this work, we follow

[6] The baryon field T_{ij} (B_{ij}) satisfies $\frac{1+\not{v}}{2} T_{ij}$ (B_{ij}) $= T_{ij}$ (B_{ij}), while $B_{ij}^{*\mu}$ satisfies $\frac{1+\not{v}}{2} B_{ij}^{*\mu} = B_{ij}^{*\mu}$ and $\gamma^\mu B_\mu^* = 0$.

the supersymmetric formation of PQχPT where the flavor group is graded [38]. Therefore Σ transforms linearly under $\mathrm{SU}(6|3)_{\mathrm{L}} \bigotimes \mathrm{SU}(6|3)_{\mathrm{R}}$,

$$\Sigma \to U_{\mathrm{L}} \Sigma U_{\mathrm{R}}^{\dagger}, \tag{18}$$

where $U_{\mathrm{L(R)}} \in \mathrm{SU}(6|3)_{\mathrm{L(R)}}$ is the left-handed (right-handed) light-flavor transformation. The operation str[ ] means supertrace over the graded light-flavor indices. The low-energy constant B_0 is related to the chiral condensate by

$$B_0 = -\frac{\langle 0|\bar{u}u + \bar{d}d|0\rangle}{f^2}, \tag{19}$$

and the quark-mass matrix in the isospin limit is

$$\mathcal{M}_q = \mathrm{diag}(m_u, m_u, m_s, m_j, m_j, m_r, m_u, m_u, m_s). \tag{20}$$

We keep the strange quark mass different from that of the up and down quarks in the valence, sea, and ghost sectors. Analogous to QCD, the strong $\mathrm{U}(1)_A$ anomaly can give rise to the large mass of the singlet field $\Phi_0 = \mathrm{str}(\Phi)/\sqrt{6}$, i.e. same size of the chiral symmetry breaking scale, and thus Φ_0 can be integrated out, resulting in residual hairpin structures in the two-point correlation function of neutral mesons [47, 48].

The Goldstone mesons couple to the above B meson and single-b baryon fields via the field ξ, which transforms as

$$\xi \to U_{\mathrm{L}} \xi U^{\dagger} = U \xi U_{\mathrm{R}}^{\dagger}, \tag{21}$$

where U is a function of U_{L}, U_{R}, and Φ. The field ξ can be used to construct the vector and axial-vector fields of meson,

$$V^{\mu} = \frac{i}{2}[\xi^{\dagger}\partial^{\mu}\xi + \xi\partial^{\mu}\xi^{\dagger}],\ A^{\mu} = \frac{i}{2}[\xi^{\dagger}\partial^{\mu}\xi - \xi\partial^{\mu}\xi^{\dagger}]. \tag{22}$$

As the vector field plays a role similar to a gauge field, the chiral covariant derivatives which act on B meson and single-b baryon fields can be defined as

$$\begin{aligned}
&\mathcal{D}^{\mu} H_i^{(\bar{b})} = \partial^{\mu} H_i^{(\bar{b})} - i(V^{\mu})_i{}^j H_j^{(\bar{b})}, \\
&\mathcal{D}^{\mu} T_{ij} = \partial^{\mu} T_{ij} - i(V^{\mu})_i{}^k T_{kj} - i(-1)^{\eta_i(\eta_j+\eta_k)}(V^{\mu})_j{}^k T_{ik}, \\
&\mathcal{D}^{\mu} S_{ij}^{\nu} = \partial^{\mu} S_{ij}^{\nu} - i(V^{\nu})_i{}^k S_{kj}^{\nu} - i(-1)^{\eta_i(\eta_j+\eta_k)}(V^{\mu})_j{}^k S_{ik}^{\nu},
\end{aligned}$$

The LO effective Lagrangian in the chiral and $1/M_B$ expansions is

$$\begin{aligned}\mathcal{L}^{(\mathrm{LO})}_{\mathrm{HH}\chi\mathrm{PT}} &= -i\mathrm{tr}_D[\bar{H}^{(\bar{b})i}v\cdot\mathcal{D}H^{(\bar{b})}_i] - i(\bar{S}^\mu v\cdot\mathcal{D}S_\mu) + i(\bar{T}v\cdot\mathcal{D}T) + \Delta^{(B)}(\bar{S}^\mu S_\mu) \\ &\quad + g_1\mathrm{tr}_D[H^{(\bar{b})}_i\bar{H}^{(\bar{b})j}\gamma_\mu\gamma_5 A^{\mu,i}_j] + ig_2\epsilon_{\mu\nu\sigma\rho}(\bar{S}^\mu v^\nu A^\sigma S^\rho) + \sqrt{2}g_3\left[(\bar{T}A^\mu S_\mu) + (\bar{S}^\mu A_\mu T)\right],\end{aligned} \tag{23}$$

where tr_D is the trace over Dirac space and v_μ is the velocity of the heavy hadrons. Note that the B-meson fields are of mass dimension 3/2 like the single-b baryon fields by absorbing $\sqrt{M_B}$ into $H^{(\bar{b})}_i$, where M_B is the mass of the B meson. The flavor index contractions of the operators for the baryons are [49]

$$\begin{aligned}(\bar{T}YT) &= \bar{T}^{ji}Y^\ell_i T_{\ell j}, \\ (\bar{S}^\mu Y S_\mu) &= \bar{S}^{\mu,ji}Y^\ell_i S_{\mu,\ell j}, \\ (\bar{T}Y^\mu S_\mu) &= \bar{T}^{ji}Y^{\mu,\ell}_i S_{\mu,\ell j}.\end{aligned} \tag{24}$$

The parameter $\Delta^{(B)}$ is the mass difference between the S and T fields with same light flavor indices,

$$\Delta^{(B)} = M_S - M_T, \tag{25}$$

which is of $O(\Lambda_{QCD})$ and does not vanish either in the chiral limit or in the heavy-quark limit.

In one-loop chiral calculations, the effects of SU(6|3) flavor symmetry breaking appear through the mass differences of hadron fields:

$$\begin{aligned}\mathcal{L}^{(\chi)}_{\mathrm{HH}\chi\mathrm{PT}} &= \tilde{\lambda}_1\mathrm{tr}_D[\bar{H}^{(\bar{b})}_i\mathcal{M}^i_{\xi,j}H^{(\bar{b})j}] + \lambda'_1\mathrm{tr}_D[\bar{H}^{(\bar{b})}_i H^{(\bar{b})i}]\mathrm{str}(\mathcal{M}_\xi) \\ &\quad + \tilde{\lambda}_2(\bar{S}^\mu\mathcal{M}_\xi S_\mu) + \lambda'_2(\bar{S}^\mu S_\mu)\mathrm{str}(\mathcal{M}_\xi) + \tilde{\lambda}_3(\bar{T}\mathcal{M}_\xi T) + \lambda'_3(\bar{T}T)\mathrm{str}(\mathcal{M}_\xi),\end{aligned} \tag{26}$$

where

$$\mathcal{M}_\xi = B_0\left(\xi\mathcal{M}^\dagger\xi + \xi^\dagger\mathcal{M}\xi^\dagger\right). \tag{27}$$

The terms proportional to λ' cause a universal shift to the single-b hadron masses, while the terms proportional to $\tilde{\lambda}$ attribute to the mass differences,

$$\begin{aligned}\delta^{(M)}_{k,\ell} &= M_{P_\ell} - M_{P_k} = M_{P^*_\ell} - M_{P^*_k} = 2\tilde{\lambda}_1 B_0(m_\ell - m_k), \\ \delta^{(B)}_{k,\ell} &= M_{\mathcal{T}_{\ell j}} - M_{\mathcal{T}_{kj}} = M_{\mathcal{S}_{\ell j}} - M_{\mathcal{S}_{kj}} = 2\tilde{\lambda}_2 B_0(m_\ell - m_k),\end{aligned} \tag{28}$$

where j represents the spectator quark and we assume $\tilde{\lambda}_2 = \tilde{\lambda}_3$. We also consider the effects of heavy-quark spin symmetry breaking at $O(\Lambda_{QCD}/m_Q)$,

$$\frac{\alpha}{m_b}\mathrm{tr}_D\left(\bar{H}_i^{(\bar{b})}\sigma_{\mu\nu}H^{(\bar{b}),i}\sigma^{\mu\nu}\right), \tag{29}$$

which vanishes in the heavy-quark limit. The α term provides the mass difference between the P^* and P mesons with same light flavor,

$$\Delta^{(M)} = M_{P_i^*} - M_{P_i} = -8\frac{\alpha}{m_b}. \tag{30}$$

In principle, there are also analogous heavy-quark spin symmetry breaking terms in the baryon sector, resulting in mass differences between B_{ij} and $B_{ij}^{*\mu}$ baryons in Eq. 14. However, we neglect these mass differences which are numerically much smaller than $\Delta^{(B)}$ [50]. If we redefine the field in which the heavy-light meson and T baryon containing u or d valence quarks are massless, the denominators of the propagators for other heavy-light mesons and single-b baryons are shifted by the linear combinations of various mass differences in Eq. 25, Eq. 28, and Eq. 30.

III. $\Delta B = 0$ FOUR-QUARK OPERATORS IN HEAVY HADRON CHIRAL PERTURBATION THEORY

In the partially quenched theory, the four-quark operators in Eq. 5 transform as left-flavor singlet, a 30-dimensional representation, and left-flavor octet, a 51-dimensional representation, built form the tensor product of two fundamental representations of SU(6|3). For lattice QCD, a more convenient form of the $\Delta B = 0$ four-quark operators can be obtained by accounting for the graded light-flavor transformations:[7]

$$\mathcal{O}^{\lambda_k^{\mathrm{PQ}}} = \mathrm{str}\left(\lambda_k^{\mathrm{PQ}}\mathcal{O}\right) + \delta^{\mathrm{eye}}\mathrm{str}\left(\lambda_k^{\mathrm{PQ}}\right)\mathrm{str}\left(\mathcal{O}\right), \tag{31}$$

with

$$\mathcal{O}^a{}_b = \bar{b}\Gamma^{(1)}q_L^a\bar{q}_{L,b}\Gamma^{(2)}b, \tag{32}$$

[7] In SU($K+N|K$) PQQCD with arbitrary K (valence and ghost quarks) and N (sea quarks), the singlet four-quark operators do not match those of unquenched QCD [51]. When the number of valence quarks is equal to the number of sea quarks (i.e $K = N = 3$ in our case), however, this mismatch disappears and the LO low-energy constants appearing in both theories are exactly same.

where

$$q_L^a = \frac{1-\gamma_5}{2} q^a, \text{ and } \bar{q}_{L,b} = \bar{q}_b \frac{1+\gamma_5}{2}. \tag{33}$$

Here $\Gamma^{(1)}$ and $\Gamma^{(2)}$ are the appropriate spin and color matrices. Following the standard construction of the operators from heavy hadron fields, we can consider $\Gamma^{(1)}$ and $\Gamma^{(2)}$ as spurious fields. To make the operators invariant under SU(2) heavy-quark spin and SU(6|3) flavor transformations, the spurious fields must transform as

$$\Gamma^{(1)} \longrightarrow S_h \Gamma^{(1)} U_L^\dagger, \qquad \Gamma^{(2)} \longrightarrow U_L \Gamma^{(2)} S_h^\dagger. \tag{34}$$

The symbol $\delta^{\rm eye}$ denotes the contribution of the eye-contractions, where the light quarks in the four-quark operators $\mathcal{O}$ are contracted by themselves, while the symbol $\lambda^{\rm PQ}$ denotes the partially-quenched extension of the Gell-Mann matrix. It is convenient to classify the operators according to three types of quarks, (valence, sea, ghost), transform under the chiral rotation of $\mathrm{SU}(3)_{\rm val} \bigotimes \mathrm{SU}(3)_{\rm sea} \bigotimes \mathrm{SU}(3)_{\rm ghost}$; the Gell-Mann matrices can be extended in a simple way, $\lambda_k^{\rm PQ} = \lambda_k \bigotimes \mathrm{diag}(1, \lambda^{\rm sea}, 1)$, where $\lambda_0 = \mathrm{diag}(1,1,1)$ for the flavor-singlet and $\lambda_3 = \mathrm{diag}(1,-1,0)$, $\lambda_8 = \mathrm{diag}(1,1,-2)$ for the flavor-octet. Here, we have introduced the symbol $\lambda^{\rm sea}$ to distinguish the disconnected (non-valence) contributions from the connected (valence) ones, i.e. $\lambda^{\rm sea} = 1$ or $\lambda^{\rm sea} = 0$ depending whether the disconnected contributions are included or not.

The LO operators in HHχPT relevant to the four-quark operators in Eq. 31 can be written as

$$\tilde{\mathcal{O}}^{\lambda_k^{\rm PQ}} = \mathrm{str}\left(\lambda_k^{\rm PQ} \tilde{\mathcal{O}}\right) + \delta^{\rm eye} \mathrm{str}\left(\lambda_k^{\rm PQ}\right) \mathrm{str}\left(\tilde{\mathcal{O}}^{(\rm bare)}\right), \tag{35}$$

where the tilded operators $\tilde{\mathcal{O}}$ for heavy-light mesons and single-b baryons are defined in below Sec. III A and Sec. III B, respectively.[8] At the tree level in the chiral expansion, the first term corresponds to connected diagrams, while the second term corresponds to disconnected diagrams which are absent for the octet. Notice that, as will be seen in Sec. IV, the first term generates disconnected diagrams as well as connected ones at the next-to-leading-order (NLO) one-loop level.

[8] The operator $\tilde{O}^{(\rm bare)}$ is the tree-level operator of $\tilde{O}$, i.e. the four-quark operators are not dressed by Goldstone mesons.

A. $\Delta B = 0$ four quark operators for heavy-light B-mesons

The most general bosonized form of the four-quark operators for heavy-light B-mesons in HHχPT is[9]

$$\begin{aligned}\left(\tilde{\mathcal{O}}_i^{\rm HM}\right)^a_{\ b} = \sum_x \Big\{ & \alpha^{(1)}_{i,x}[(\xi\bar{H}^{(b)})^a\Gamma^{(1)}\Xi_x][\Gamma^{(2)}(H^{(b)}\xi^\dagger)_b\Xi'_x] + \alpha^{(2)}_{i,x}[(\xi\bar{H}^{(b)})^a\Gamma^{(1)}\Xi_x\Gamma^{(2)}(H^{(b)}\xi^\dagger)_b\Xi'_x] \\ & + \alpha^{(3)}_{i,x}[(\xi H^{(\bar{b})})^a\Gamma^{(1)}\Xi_x][\Gamma^{(2)}(\bar{H}^{(\bar{b})}\xi^\dagger)_b\Xi'_x] + \alpha^{(4)}_{i,x}[(\xi H^{(\bar{b})})^a\Gamma^{(1)}\Xi_x\Gamma^{(2)}(\bar{H}^{(\bar{b})}\xi^\dagger)_b\Xi'_x] \\ & + \alpha^{(5)}_{i,x}[(\xi\bar{H}^{(b)})^a(H^{(b)}\xi^\dagger)_b\Xi_x][\Gamma^{(2)}\Gamma^{(1)}\Xi'_x] + \alpha^{(6)}_{i,x}[(\xi\bar{H}^{(b)})^a(H^{(b)}\xi^\dagger)_b\Xi_x\Gamma^{(2)}\Gamma^{(1)}\Xi'_x] \\ & + \alpha^{(7)}_{i,x}[(\xi H^{(\bar{b})})^a(\bar{H}^{(\bar{b})}\xi^\dagger)_b\Xi'_x][\Gamma^{(2)}\Gamma^{(1)}\Xi'_x] + \alpha^{(8)}_{i,x}[(\xi H^{(\bar{b})})^a(\bar{H}^{(\bar{b})}\xi^\dagger)_b\Xi'_x\Gamma^{(2)}\Gamma^{(1)}\Xi'_x]\Big\},\end{aligned} \tag{36}$$

where $i = 1, 2, 3, 4$, and Ξ_x are Ξ'_x are all possible pairs of Dirac structures [10]. The bracket notation [ ] represents the trace over the Dirac space. Any insertion of $\not{v}$ in the Dirac structures can be absorbed by the heavy meson fields, $\not{v}H(v) = H(v)$, while any insertion of γ_5 at most changes the sign of Γ. The HQET parity conservation and the contraction of Lorentz indices requires that $\Xi_x = \Xi'_x$. The single Dirac-trace terms can be rewritten by the double trace using the 4×4 matrix identity

$$4[AB] = [A][B] + [\gamma_5 A][\gamma_5 B] + [A\gamma_\mu][\gamma^\mu B] + [A\gamma_\mu\gamma_5][\gamma_5\gamma^\mu B] + \frac{1}{2}[A\sigma_{\mu\nu}][\sigma^{\mu\nu}]. \tag{37}$$

Since $\Gamma^{(1)}$ and $\Gamma^{(2)}$ are left- and right-handed current respectively, the last four terms in Eq. 36 vanish. In summary, the operators in $\tilde{\mathcal{O}}_i^{\rm HM}$ can be reduced to

$$\begin{aligned}\left(\tilde{\mathcal{O}}_i^{\rm HM}\right)^a_{\ b} = \sum_x \Big\{ & \bar{\alpha}_{i,x}[(\xi\bar{H}^{(b)})^a\Gamma^{(1)}\Xi_x][\Gamma^{(2)}(H^{(b)}\xi^\dagger)_b\Xi_x] \\ & + \alpha_{i,x}[(\xi H^{(\bar{b})})^a\Gamma^{(1)}\Xi_x][\Gamma^{(2)}(\bar{H}^{(\bar{b})}\xi^\dagger)_b\Xi_x]\Big\},\end{aligned} \tag{38}$$

where $\Xi_x \in \{1, \gamma_\nu, \sigma_{\nu\rho}\}$. After evaluating the trace over the Dirac space, we obtain

$$\begin{aligned}\left(\tilde{\mathcal{O}}_i^{\rm HM}\right)^a_{\ b} = & \ \bar{\beta}_{i,1}(\xi P^{(b)\dagger})^a(P^{(b)}\xi^\dagger)_b + \bar{\beta}_{i,2}(\xi P^{*(b)\dagger}_\mu)^a(P^{*(b),\mu}\xi^\dagger)_b \\ & + \beta_{i,1}(\xi P^{(\bar{b})})^a(P^{(\bar{b})\dagger}\xi^\dagger)_b + \beta_{i,2}(\xi P^{*(\bar{b})}_\mu)^a(P^{*(\bar{b})\dagger,\mu}\xi^\dagger))_b,\end{aligned} \tag{39}$$

---

[9] The field $H_i^{(b)}$ for mesons containing a b quark and a light anti-quark of flavor i is obtained by applying the charge conjugation operation to the field $H_i^{(\bar{b})}$ in Eq. (7): $H_i^{(b)} = \frac{1+\not{v}}{2}\left(P^{*(b)}_{i,\mu}\gamma^\mu - P_i^{(b)}\gamma_5\right)$, which transforms under S_h and U as $H_i^{(b)} \to S_h H_j^{(b)} U^{\dagger j}{}_i$. Also, the conjugate field is defined as $\bar{H}_i^{(b)} = \gamma^0 H_i^{(b)\dagger}\gamma^0$.

[10] The Dirac structure $\Xi_x = 1,\ \gamma_\mu,\ \sigma_{\mu\nu}$, and possible combinations with $\not{v}$ and γ_5.

where β and $\bar{\beta}$ are linear combinations of $\alpha_{i,x}$ and $\bar{\alpha}_{i,x}$, respectively. Explicitly we have, for $i = 1, 3$,

$$\begin{aligned}\beta_{i,1}(\bar{\beta}_{i,1}) &= 4\alpha_{i,1}(\bar{\alpha}_{i,1}) + 16\alpha_{i,\gamma_\nu}(\bar{\alpha}_{i,\gamma_\nu}),\\ \beta_{i,2}(\bar{\beta}_{i,2}) &= 4\alpha_{i,1}(\bar{\alpha}_{i,1}),\end{aligned} \tag{40}$$

for $i = 2, 4$

$$\begin{aligned}\beta_{i,1}(\bar{\beta}_{i,1}) &= 4\alpha_{i,1}(\bar{\alpha}_{i,1}) + 4\alpha_{i,\gamma_\nu}(\bar{\alpha}_{i,\gamma_\nu}),\\ \beta_{i,2}(\bar{\beta}_{i,2}) &= 4\alpha_{i,\gamma_\nu}(\bar{\alpha}_{i,\gamma_\nu}).\end{aligned} \tag{41}$$

As shown above, the low-energy constants (LECs) for pseudo-scalar and vector meson mixing processes are different in all cases, which is different from the results in Ref. [39] where LECs for the cases of $i = 2, 4$ are same. Since having a single LEC for the operators in an effective theory greatly simplifies chiral extrapolation of corresponding lattice data, it is important to confirm our result from another consideration. For this purpose, consider our four-fermion operators, $\mathcal{O}_{i,a}$, which appear in the HQET as,

$$\mathcal{O}_{i,a}^{\rm HQET} = Q^\dagger \Gamma^{(1)} q_a \bar{q}_a \Gamma^{(2)} Q + \tilde{Q} \Gamma^{(1)} q_a \bar{q}_a \Gamma^{(2)} \tilde{Q}^\dagger, \tag{42}$$

where Γ are the appropriate Dirac and color structures, while Q and $\tilde{Q}$ are the fields annihilating a heavy quark and heavy anti-quark, respectively. Note that these fields do not create the corresponding anti particles but their conjugate fields do.

We also consider the heavy quark spin operator [52]

$$S_Q^3 = \epsilon^{ij3}[Q^\dagger \sigma_{ij} Q - \tilde{Q}\sigma_{ij}\tilde{Q}^\dagger], \tag{43}$$

where $\sigma_{ij} = \frac{i}{2}[\gamma_i, \gamma_j]$ with $i, j = 1, 2, 3$. Since the heavy quark spin operator changes the spin of heavy-light meson by one, the relation between LECs in the operator $\tilde{\mathcal{O}}_i^{\rm HM}$ can be seen from calculating the commutation (or anti-commutation) of S_Q^3 and $\mathcal{O}_{i,0}^{\rm HQET}$ acting on the pseudo-scalar heavy-light meson state $|P\rangle$ containing a heavy-quark field Q. We find that

$$[S_Q^3, \mathcal{O}_{i,a}^{\rm HQET}]|P\rangle \neq 0, \quad \{S_Q^3, \mathcal{O}_{i,a}^{\rm HQET}\}|P\rangle \neq 0. \tag{44}$$

Similar results can be shown for the pseudo-scalar heavy-light meson state $|\bar{P}\rangle$ containing a heavy anti-quark field $\tilde{Q}$. This implies that the pseudo-scalar and vector meson mixing processes via these operators are not simply related to each other, and so they are accompanied by different LECs consistent with Eqs. 39-41.

B. $\Delta B = 0$ four quark operators for single-b baryons

The most generalized form of four-quark operators for single-b baryons in HHχPT is

$$\left(\tilde{\mathcal{O}}_i^{\rm HB}\right)^a_{\ b} = \sum_x \Big\{ \alpha'^{(1)}_{i,x} (\bar{S}_\mu \xi^\dagger)^{aj} \Gamma^{(1)} \Xi_x^{\mu\nu} \Gamma^{(2)} (\xi S_\nu)_{bj} + \alpha'^{(2)}_{i,x} (\bar{S}_\mu \xi^\dagger)^{aj} (\xi S_\nu)_{bj} {\rm tr}_{\rm D}[\Gamma^{(1)} \Xi_x^{\mu\nu} \Gamma^{(2)}] + \alpha'^{(3)}_{i,x} (\bar{T} \xi^\dagger)^{aj} \Gamma^{(1)} \Xi_x \Gamma^{(2)} (\xi T)_{bj} + \alpha'^{(4)}_{i,x} (\bar{T} \xi^\dagger)^{aj} (\xi T)_{bj} {\rm tr}_{\rm D}[\Gamma^{(1)} \Xi_x \Gamma^{(2)}] \Big\}, \quad (45)$$

where $i = 1, 2, 3, 4$, and Ξ and $\Xi^{\mu\nu}$ are all possible Dirac structures,

$$\Xi = 1,\ \not{v}, \quad \Xi^{\mu\nu} = g^{\mu\nu},\ \not{v} g^{\mu\nu},\ \sigma^{\mu\nu},\ \not{v}\sigma^{\mu\nu},\ \sigma^{\mu\nu}\not{v}, \quad (46)$$

and possible combinations with γ^5. Any insertion of γ^5 changes at most the overall sign. One may consider the terms $\bar{T}\Gamma^{(1)}\Xi_x^\mu \Gamma^{(2)} S_\mu$ and $\bar{T} S_\mu [\Gamma^{(1)} \Xi_x^\mu \Gamma^{(2)}]$ along with their conjugates which are invariant under SU(2) heavy quark spin symmetry, where $\Xi^\mu = \gamma^\mu,\ \not{v}\gamma^\mu,\ \gamma^\mu \not{v}$. However, we exclude these terms because, along with $\lambda^{\rm PQ}$, they violate the SU$(6|3)_{\rm L+R}$ flavor symmetry. By evaluating the Dirac matrices we obtain

$$\left(\tilde{\mathcal{O}}_i^{\rm HB}\right)^a_{\ b} = \left\{ \beta'_{i,1} (\bar{B}\xi^\dagger)^{aj} (\xi B)_{bj} + \beta'_{i,2} (\bar{B}^*_\mu \xi^\dagger)^{aj} (\xi B^{*\mu})_{bj} + \beta'_{i,3} (\bar{T}\xi^\dagger)^{aj} (\xi T)_{bj} \right\}, \quad (47)$$

where β''s are linear combinations of α''s. The explicit values of β''s are, for $i = 1, 3$,

$$\beta'_{i,1} = 4\alpha'^{(1)}_{i,\not{v} g^{\mu\nu}} - 8i(\alpha'^{(1)}_{i,\not{v}\sigma^{\mu\nu}} + \alpha'^{(1)}_{i,\sigma^{\mu\nu}\not{v}}),\ \beta'_{i,2} = -\frac{1}{2}\beta'_{i,1} - 2\alpha'^{(1)}_{i,\not{v} g^{\mu\nu}},\ \beta'_{i,3} = -4\alpha'^{(3)}_{i,\not{v}}, \quad (48)$$

and for $i = 2, 4$,

$$\beta'_{i,1} = -2\alpha'^{(1)}_{i,\not{v} g^{\mu\nu}} - 4i(\alpha'^{(1)}_{i,\not{v}\sigma^{\mu\nu}} + \alpha'^{(1)}_{i,\sigma^{\mu\nu}\not{v}}),\ \beta'_{i,2} = \frac{1}{2}\beta'_{i,1} + 3\alpha'^{(1)}_{i,\not{v} g^{\mu\nu}},\ \beta'_{i,3} = 2\alpha'^{(3)}_{i,\not{v}}, \quad (49)$$

Unfortunately, this result implies that none of the low-energy constants are related to each other, and thus all of them must be considered as independent parameters in fitting lattice QCD data.

IV. MATRIX ELEMENTS OF $\Delta B = 0$ OPERATORS

The generic forms of the matrix elements of $\Delta B = 0$ four-quark operators to the NLO in SU(6|3) partially quenched HHχPT can be written as

$$\langle B|\mathcal{O}^{\lambda^{\rm PQ}_k}|B\rangle = (1 + 3\lambda^{\rm sea}\delta^{\rm eye}\delta_{k0}) \left[C^k_M \beta_1 (1 + \mathcal{W}_B) + \beta_2 \mathcal{Q}^k_B\right] + \beta_1 \mathcal{T}^k_B + \text{analytical terms}, \quad (50)$$

TABLE I: Coefficients C_M^k in Eq. 50.

	C_M^k		
	B_u	B_d	B_s
$k=3$	1	-1	0
$k=8$	1	1	-2

TABLE II: Coefficients C_T^k and C_S^k in Eq. 51.

	C_T^k			C_S^k					
	Λ_b	$\Xi_b^{+\frac{1}{2}}$	$\Xi_b^{-\frac{1}{2}}$	Σ_b^0	Σ_b^+	Σ_b^-	$\Xi_b^{\prime+\frac{1}{2}}$	$\Xi_b^{\prime-\frac{1}{2}}$	Ω_b
$k=3$	0	$\frac{1}{2}$	$-\frac{1}{2}$	0	1	-1	$\frac{1}{2}$	$-\frac{1}{2}$	0
$k=8$	1	$-\frac{1}{2}$	$-\frac{1}{2}$	1	1	1	$-\frac{1}{2}$	$-\frac{1}{2}$	-2

for B mesons[11] and

$$\begin{aligned}
\langle T|\mathcal{O}_k^{\lambda^{\rm PQ}}|T\rangle &= (1+3\lambda^{\rm sea}\delta^{\rm eye}\delta_{k0})\left[C_T^k\beta_3'(1+\mathcal{W}_T)+(-\beta_1'+2\beta_2')\mathcal{Q}_T^k\right]+\beta_3'\mathcal{T}_T^k \\
&\quad +\text{analytical terms}, \\
\langle S|\mathcal{O}_k^{\lambda^{\rm PQ}}|S\rangle &= (1+3\lambda^{\rm sea}\delta^{\rm eye}\delta_{k0})\left[C_S^k\beta_1'(1+\mathcal{W}_S)+(-2\beta_1'+\beta_2')\mathcal{Q}_{S_S}^k+\beta_3'\mathcal{Q}_{S_T}^k\right]+\beta_1'\mathcal{T}_S^k \\
&\quad +\text{analytical terms}, \qquad (51)
\end{aligned}$$

for T and S baryons. The equality symbol means the matching between PQQCD and the chiral effective theory. The coefficients $C_M^0 = C_T^0 = C_S^0 = 1$ for all external single-b hadrons, while those with $k = 3, 8$ are given in Table I for B mesons and in Table II for T and S baryons.

There are three types of non-analytic one-loop contributions, the wavefunction renormalization resulting from the self-energy diagrams ($\mathcal{W}$), tadpole ($\mathcal{T}$), and sunset ($\mathcal{Q}$) diagrams, as depicted in Fig. 1. We perform these calculations both at infinite volume and on a torus of length L in each of three spatial directions (the temporal extent is assumed to be infinite),

[11] More precisely, $|B\rangle$ denotes the state annihilating a B meson containing a anti-b quark and a light quark, where we use the standard notation, e.g. $B_u = B^+ = \bar{b}u$. It is straightforward to extend our calculations to the $\Delta B = 0$ matrix elements involving mesons containing a b quark and a light antiquark.

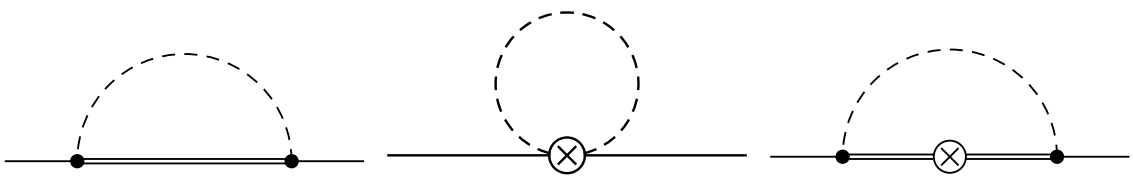

FIG. 1: One-loop diagrams contributing to the matrix elements of $\Delta B = 0$ four-quark operators. The single and double solid lines correspond to external and internal heavy hadrons, such as B, B^* mesons or T, S baryons, respectively. The dashed lines are the Goldstone meson propagators including possible hairpin interactions. The crossed circles denote the LO four-quark operators in HHχPT in Eq. 35, while the filled circles denote the axial couplings in the chiral Lagrangian in Eq. 24. Diagrams from left to right are the wavefunction renormalization, tadpole- and sunset-type operator renormalizations, respectively.

where the results are presented in Sec. IV A and Sec. IV B below. Because the $\Delta B = 0$ four-quark operators in HHχPT have the same forms for any values of i as in Eq. 39 and Eq. 47, the one-loop chiral corrections are independent on the structure of the $\Delta B = 0$ operators in Eq. 5 and thus we omit the subscript i throughout this section for convenience.

The analytic terms include the NLO contributions of chiral symmetry breaking effects $\sim m_\phi^2$ and heavy quark symmetry breaking effects $\sim \Lambda_{QCD}/m_b$. In the chiral expansion, in particular, the former contributions play a role of counterterms which are necessary to renormalize the one-loop contributions. There are five corresponding NLO operators, $\mathrm{str}\left(\lambda_k^{\mathrm{PQ}}\mathcal{M}_\xi\tilde{\mathcal{O}}\right)$, $\mathrm{str}\left(\lambda_k^{\mathrm{PQ}}\tilde{\mathcal{O}}\right)\mathrm{str}(\mathcal{M}_\xi)$, $\mathrm{str}\left(\lambda_k^{\mathrm{PQ}}\mathcal{M}_\xi\right)\mathrm{str}\left(\tilde{\mathcal{O}}\right)$, $\mathrm{str}\left(\lambda_k^{\mathrm{PQ}}\right)\mathrm{str}\left(\tilde{O}\mathcal{M}_\xi\right)$, and $\left(\lambda_k^{\mathrm{PQ}}\right)\mathrm{str}\left(\tilde{O}\right)\mathrm{str}(\mathcal{M}_\xi)$, accompanying with unknown low-energy constants. Notice that in the isospin and QCD limit the last three operators for λ_3^{PQ} vanish, while those for λ_8^{PQ} are proportional to $m_K^2 - m_\pi^2$ originate from the flavor SU(3) symmetry breaking.

A. One-loop contributions for B Meson

First, we study the one-loop contributions for B mesons in Eq. 50. To take account of the flavor SU(3) breaking effects from both the Goldstone masses and the heavy-meson spectrum, we investigate the structure of the one-loop diagrams by analyzing the quark-flavor flow picture [53]. To do this, we define the rules as below.

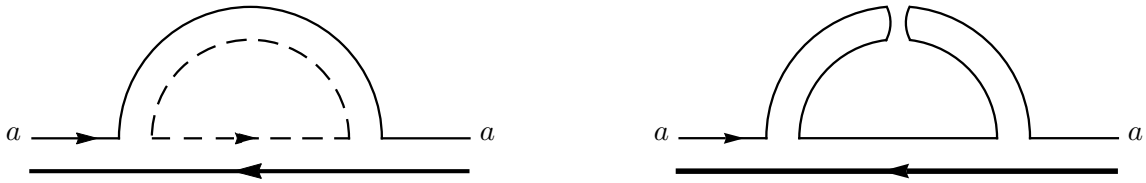

(a) (b)

FIG. 2: Self-energy diagrams contributing to the matrix elements containing B mesons. The solid thick and thin lines denote the anti-b quark and the valence light quark, respectively, while the dashed thin line denotes the sea light quark. Diagram (b) is the hairpin structure.

- Each flavor flow line in a one-loop diagram has a direction and a flavor index: the flow along the direction means a quark with that flavor, while the flow against the direction means its antiquark. We drop the flavor index of a b-quark because of its irrelevance to our discussion.

- The "tilded" coefficients are for the hairpin contributions from the flavor-neutral mesons.

- The "bar" notation in the coefficients denotes the flavor-disconnected diagrams appearing in the chiral expansion, which are distinguished from the eye-contraction in Eq. 35.

Following the above rules and the quark flow picture in Fig. 2, the wave-function renormalization contributions can be written as [36]

$$\mathcal{W}_{B_a} \;=\; \frac{ig_1^2}{f^2}\left[6\mathcal{H}(M_{a,j},\Delta^{(M)}+\delta^{(M)}_{a,j})+3\mathcal{H}(M_{a,r},\Delta^{(M)}+\delta^{(M)}_{a,r})-\tilde{\mathcal{H}}(M_{a,a},\Delta^{(M)})\right], \quad (52)$$

where a runs over the valence light-quark flavors. The non-analytic functions $\mathcal{H}$ and $\tilde{\mathcal{H}}$ are defined in the Appendix A, while the mass parameters $M_{a,b}$, $\Delta^{(M)}$ and $\delta^{(M)}_{a,b}$ are defined in Sec. II.

The loop contributions for tadpole integrals are completely determined by the structure of the operators $\tilde{\mathcal{O}}^{\rm HM}$ in Eq. 39, where the flavor SU(3) breaking effects arise solely from the Goldstone masses. As a result, we obtain

$$\mathcal{T}^k_B \;=\; \frac{i}{f^2}\sum_{\phi}(x^{B,k}_{\phi_{ab}}+\lambda^{\rm sea}\bar{x}^{B,k}_{\phi_{ab}})\mathcal{I}(M_{a,b}), \quad (53)$$

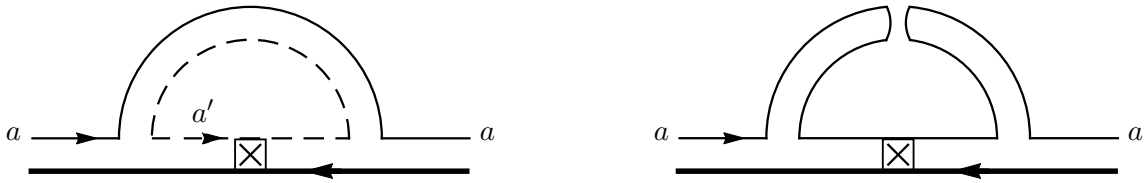

FIG. 3: Sunset diagrams contributing to the matrix elements containing B mesons. The solid thick and thin lines denote the anti-b quark and the valence light quark, respectively. The crossed square is the operator $\tilde{\mathcal{O}}^{\lambda_k^{\rm PQ}}$. Diagram (b) is the hairpin structure.

where the summation runs over all possible Goldstone mesons in SU(6|3) PQχPT. The non-analytic function I is defined in Appendix A and the coefficients x and $\bar{x}$ are given in Table III in Appendix B. Notice that all hairpin diagrams cancel out and do not contribute to any one-loop tadpole corrections.

The quark flow picture for sunset diagrams is presented in Fig. 3, where the crossed square represents the operator $\tilde{\mathcal{O}}^{\lambda_k^{\rm PQ}}$ including both the eye- and noneye-contraction in Eq. 35. The hairpin diagrams for the noneye-contraction give rise to the connected contribution, while the others give rise to the disconnected contribution. The contributions from the sunset diagrams are then summarized as

$$\mathcal{Q}_B^k \;=\; \frac{ig_1^2}{f^2}\left[\sum_{\phi}\lambda^{\rm sea}\bar{y}^{B,k}_{\phi_{ab}}\mathcal{H}(M_{a,b},\Delta^{(M)}+\delta^{(M)}_{a,b}) - \sum_{\phi\phi'}\tilde{y}^{B,k}_{\phi_{aa}\phi'_{bb}}\tilde{\mathcal{H}}(M_{a,b},\Delta^{(M)})\right], \qquad (54)$$

where the second term sums over all pairs of flavor-neutral states in the valence-valence sector, i.e. $\phi\phi'$ runs over $\eta_u\eta_u$, $\eta_u\eta_s$, and $\eta_s\eta_s$. The coefficients are given in Table IV in Appendix B.

B. One-loop contributions for single-b Baryon

To discuss the structure of the single-b baryon one-loop diagrams within the quark-flavor flow picture, we introduce one more rule:

- The "primed" coefficients are for the one-loop diagrams involving the internal T baryon, while the unprimed coefficients for the diagrams involving the internal S baryon.

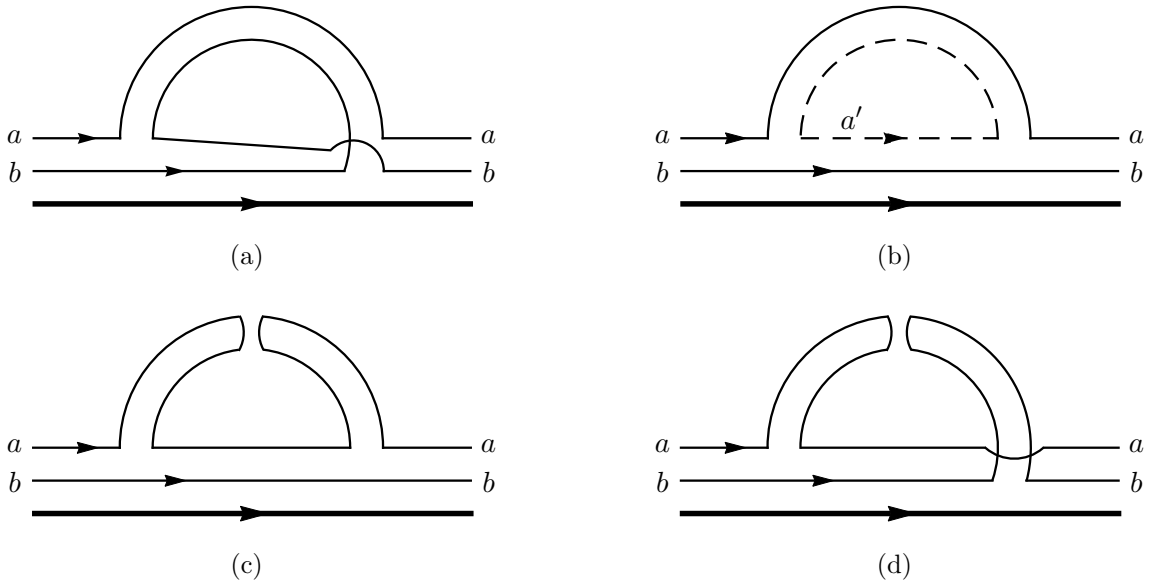

FIG. 4: Self-energy diagrams contributing to the matrix elements containing single-b baryons. The solid thick and thin lines denote the anti-b quark and the valence light quark, respectively, while the dashed thin line denotes the sea light quark. Diagram (c) and (b) are the hairpin structures. The diagrams including the internal S baryons lead to terms multiplied by w and $\tilde{w}$, while those including the internal T baryons lead to terms multiplied by w' and $\tilde{w}'$ in Eq. 55, where the tilded coefficients denote the hairpin structure. The diagrams obtained by interchanging the flavor indices a and b , not shown in this figure, have also been taken into account in our results in Table V.

In Fig. 4, we show the quark-flavor flow picture for the baryon self-energy diagrams. Following the above rule and the rules defined in Sec. IV A, we obtain the contributions from the wavefunction renormalization for T and S baryons [37, 46],

$$\begin{aligned}
\mathcal{W}_T &= \frac{ig_3^2}{f^2}\left[\sum_{\phi} w^T_{\phi_{ab}}\mathcal{H}(M_{a,b},\Delta^{(B)}+\delta^{(B)}_{a,b}) - \sum_{\phi\phi'}\tilde{w}^T_{\phi_{aa}\phi'_{bb}}\tilde{\mathcal{H}}(M_{a,b},\Delta^{(B)})\right], \\
\mathcal{W}_S &= \frac{ig_2^2}{f^2}\left[\sum_{\phi} w^S_{\phi_{ab}}\mathcal{H}(M_{a,b},\delta^{(B)}_{a,b}) - \sum_{\phi\phi'}\tilde{w}^S_{\phi_{aa}\phi'_{bb}}\tilde{\mathcal{H}}(M_{a,b},0)\right] \\
&\quad + \frac{ig_3^2}{f^2}\left[\sum_{\phi} w'^S_{\phi_{ab}}\mathcal{H}(M_{a,b},-\Delta^{(B)}+\delta^{(B)}_{a,b}) - \sum_{\phi\phi'}\tilde{w}'^S_{\phi_{aa}\phi'_{bb}}\tilde{\mathcal{H}}(M_{a,b},-\Delta^{(B)})\right], \qquad (55)
\end{aligned}$$

where the summations are over the Goldstone mesons in SU(6|3) PQχPT. The coefficients $w, w', \tilde{w}$, and $\tilde{w}'$ are presented in Table V in Appendix C, while the mass parameters $\Delta^{(B)}$ and $\delta^{(B)}_{a,b}$ are defined above in Sec. II.

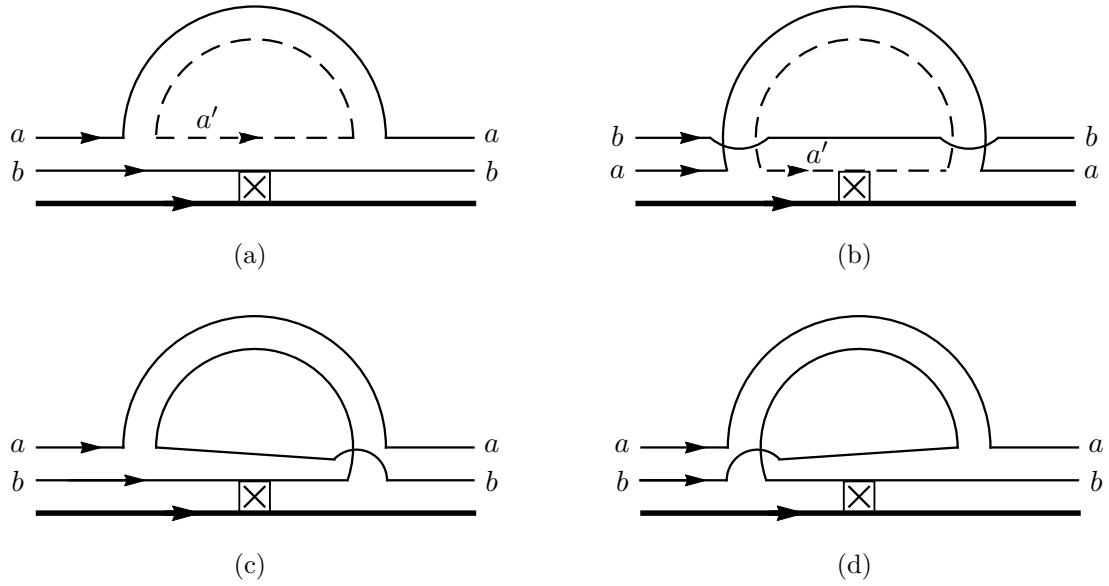

FIG. 5: Sunset diagrams contributing to the $\Delta B = 0$ matrix element of single-b baryons without the hairpin structure. The solid thick and thin lines denote the anti-b quark and the valence light quark, respectively, while the dashed thin line denotes the sea light quark. The crossed square is the operator $\tilde{\mathcal{O}}^{\lambda_k^{\rm PQ}}$. Diagram (b) contributes to the $\bar{y}$ terms, while the diagrams including the internal S and T baryons lead to terms multiplied by y and y' in Eq. 58, respectively. The diagrams obtained by interchanging the flavor indices a and b , not shown in this figure, have also been taken into account in our results in Table VII, Table VIII and Table IX.

A single-b baryon carries two light-flavor quarks, where one of them is contracted with the four-quark operators, while the other is the spectator quark. Therefore, the situation for the baryon tadpole and sunset diagrams is more involved compared to those for the meson diagrams. We first obtain the contributions from tadpole diagrams,

$$\mathcal{T}^k_{T(S)} = \frac{i}{f^2}\sum_{\phi}(x^{T(S),k}_{\phi_{ab}} + \lambda^{\rm sea}\bar{x}^{T(S),k}_{\phi_{ab}})\mathcal{I}(M_{a,b}), \tag{56}$$

where the coefficients $x^{T(S)}$ and $\bar{x}^{T(S)}$ are given in Table VI in Appendix C. Like the case of B mesons, all hairpin diagrams cancel out and do not contribute to any one-loop tadpole corrections.

The quark-flavor flow structure for the baryon sunset diagrams can be summarized in Figs. 5 and 6. Notice that the four-quark operators do not change the spin of a single-b baryon as discussed in Sec. III, and thus there are only three possible combinations of internal baryons, $T_{aj} - T_{bj}$, $B_{aj} - B_{bj}$, and $B^*_{aj} - B^*_{bj}$; the flavor indices a and b are contracted with $\lambda_k^{\rm PQ}$, while

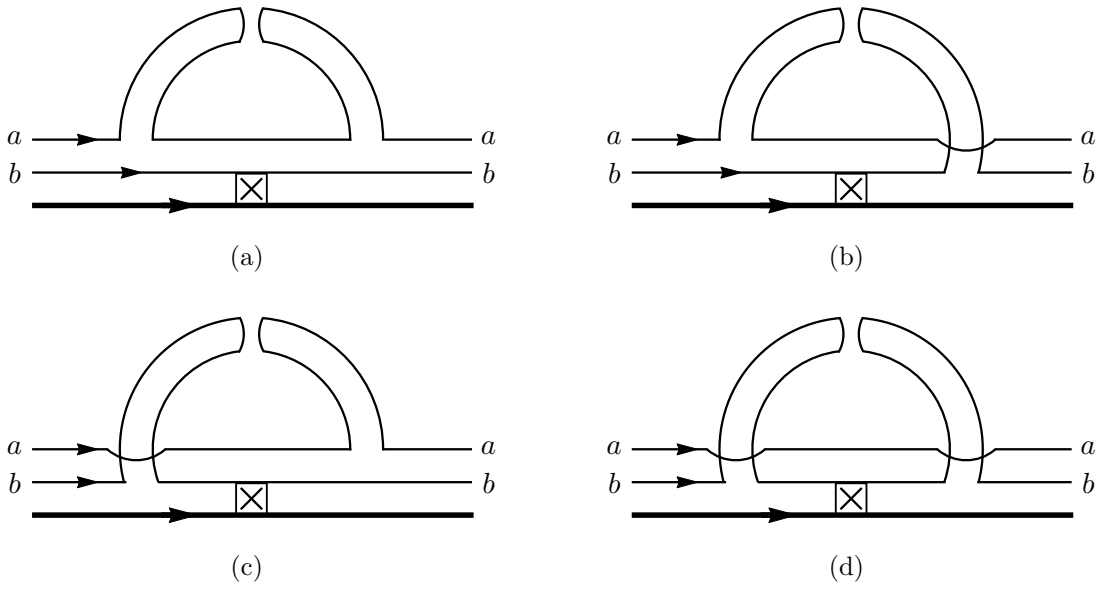

FIG. 6: Sunset diagrams contributing to the $\Delta B = 0$ matrix element of single-b baryons involving the hairpin structure. The solid thick and thin lines denote the anti-b quark and the valence light quark, respectively, while the dashed thin line denotes the sea light quark. The crossed square is the operator $\tilde{\mathcal{O}}^{\lambda_k^{\rm PQ}}$. The diagrams including the internal S and T baryons lead to terms multiplied by $\tilde{y}$ and $\tilde{y'}$ in Eq. 58, respectively. The diagrams obtained by interchanging the flavor indices a and b, not shown in this figure, have also been taken into account in our results in Table VII, Table VIII and Table IX.

the index j is for the spectator quark. For the noneye-contraction, both nonhairpin and hairpin diagrams can give rise to the connected contribution to the matrix elements; the nonhairpin diagram in Fig. 5b is the only one giving rise to the disconnected contribution. The contributions from the sunset diagrams for T and S baryons are summarized as

$$\begin{aligned}
\mathcal{Q}_T^k &= \frac{ig_3^2}{f^2}\left[\sum_\phi (y_{\phi_{ab}}^{T,k} + \lambda^{\rm sea}\bar{y}_{\phi_{ab}}^{T,k})\mathcal{H}(M_{a,b}, \Delta^{(B)} + \delta_{a,b}^{(B)}) - \sum_{\phi\phi'} \tilde{y}_{\phi_{aa}\phi'_{bb}}^{T,k}\tilde{\mathcal{H}}(M_{a,b}, \Delta^{(B)})\right], \\
\mathcal{Q}_{S_S}^k &= \frac{ig_2^2}{3f^2}\left[\sum_\phi (y_{\phi_{ab}}^{S,k} + \lambda^{\rm sea}\bar{y}_{\phi_{ab}}^{S,k})\mathcal{H}(M_{a,b}, \delta_{a,b}^{(B)}) - \sum_{\phi\phi'} \tilde{y}_{\phi_{aa}\phi'_{bb}}^{S,k}\tilde{\mathcal{H}}(M_{a,b}, 0)\right], \\
\mathcal{Q}_{S_T}^k &= \frac{ig_3^2}{f^2}\left[\sum_\phi (y'^{S,k}_{\phi_{ab}} + \lambda^{\rm sea}\bar{y}'^{S,k}_{\phi_{ab}})\mathcal{H}(M_{a,b}, -\Delta^{(B)} + \delta_{a,b}^{(B)}) - \sum_{\phi\phi'} \tilde{y}'^{S,k}_{\phi_{aa}\phi'_{bb}}\tilde{\mathcal{H}}(M_{a,b}, -\Delta^{(B)})\right],
\end{aligned} \tag{57}$$

where the summations are over the Goldstone mesons in SU(6|3) PQχPT. The coefficients $y, y', \bar{y}, \bar{y}', \tilde{y}$ and $\tilde{y}'$ are presented in Table VII, Table VIII and Table IX in Appendix C.

C. Evaluation of one-loop contributions

In this subsection, we evaluate the one-loop diagrams including external B_d, B_s mesons, and Λ_b baryon to provide insight on chiral extrapolations of the matrix elements obtained from lattice simulations. As seen in Eqs. 50 and 51, the matrix elements of the singlet four-quark operators are complicated by the eye-contraction. For this reason, we restrict our attention to the matrix elements of the octet operators. We carry out the calculations in the QCD limit, where the masses of sea quarks are same with their counter part valence quarks. We fix $f = 0.132$ GeV, $\Delta^{(M)} = 45$ MeV, $\Delta^{(B)} = 200$ MeV, $M_{s,s} = 691$ MeV, $\tilde{\lambda}_1 = 0.189$ GeV^{-1}, and $\tilde{\lambda}_2 = 0.377$ GeV^{-1} [12]. We also fix the renomalization scale by $\mu = 4\pi f$. The numerical values of the axial couplings g_1 and g_3 are taken from the recent lattice QCD calculations [55, 56] as follows: $0.398 < g_1 < 0.5$ and $0.58 < g_3 < 0.84$ with central values of $g_1 = 0.449$ and $g_3 = 0.71$, respectively. We also vary the ratios of P^* to P and S to T LECs over the reasonable ranges, $|\beta_2/\beta_1| < 2$ for B mesons and $|(-\beta_1' + 2\beta_2')/\beta_3'| < 2$ for Λ_b.

We first consider SU(3) theory in the isospin limit. The typical one-loop contributions involve kaons or η-mesons, where their chiral logarithms in the SU(2) chiral limit are given as $(M_K^2/\mu^2)\log(M_K^2/\mu^2) \sim 0.21$ or $(M_\eta^2/\mu^2)\log(M_\eta^2/\mu^2) \sim 0.25$. Using the pion mass over the typical range of 200 MeV $\leq M_\pi \leq$ 400 MeV and the standard subtraction scheme in Eq. A1, we find that the size of one-loop contributions is comparable with the LO matrix elements. Therefore, the convergence of the SU(3) chiral expansion of the matrix elements becomes questionable. Fortunately, for chiral extrapolations of lattice results one only requires knowledge of the pion mass dependence, and this can be achieved within SU(3) theory by taking the subtraction scheme below inspired by SU(2) chiral perturbation theory, where the one-loop chiral logarithms vanish in the SU(2) chiral limit [37, 57, 58]. Notice that the use of different subtraction schemes in one-loop integrals results in the finite renormalization of the LO matrix elements, but does not change physical quantities such as the hadron masses. We define the non-analytic functions $I^{\rm sub}(m)$ and $H^{\rm sub}(m, \Delta)$, which are relevant

[12] The values of $\Delta^{(M)}$ and $\Delta^{(B)}$ are consistent with experiment. The value of $M_{s,s}$ is determined by the Gell-Mann-Okubo formulas using $(M_K)_{\rm phys} = 0.498$ GeV and $(M_\pi)_{\rm phys} = 0.135$ GeV, while the values of $\tilde{\lambda}_1$ and $\tilde{\lambda}_2$ are determined by Eq. 28 using $(M_{B_s})_{\rm phys} - (M_{B_d})_{\rm phys} = 0.087$ GeV and $(M_{\Xi^0})_{\rm phys} - (M_{\Lambda_b^0})_{\rm phys} = 0.173$ GeV, respectively. The physical values of hadron masses used in the determination of these various parameters are found in Ref. [54].

to the one-loop calculations, as

$$\begin{aligned} I^{(\mathrm{sub})}(m) &= I(m) - I(m_0), \\ H^{(\mathrm{sub})}(m,\Delta) &= H(m,\Delta) - H(m_0,\Delta_0), \end{aligned} \tag{58}$$

where m_0 and Δ_0 are the mass of Goldstone mesons and the mass difference between external and internal single-b hadrons at zero pion mass, respectively. We recall that the mass of a Goldstone meson is written as $M_{a,b}^2 = B_0(m_a + m_b)$, i.e. $M_K^2 = (M_{s,s}^2 + M_\pi^2)/2$ and $M_\eta^2 = (2M_{s,s}^2 + M_\pi^2)/3$, and the strange quark mass $M_{s,s}$ is fixed. The above non-analytic functions involve logarithms of the masses of Goldstone mesons, where for kaons and η-mesons these logarithms[13] are much less sensitive to the pion mass than those for pions are. Note that the subtracted terms are constants and appropriately absorbed by the counterterms.

Our current understanding on the matrix elements are very limited; see Ref. [16] for the summary of previous determinations. In particular, there are only a few quenched lattice simulations in Ref. [9, 10] for B mesons and in Ref. [11] for Λ_b. Instead of using the definite values of the LECs β_1 and β_3', therefore, we rather calculate the NLO one-loop contributions normalized by the LO LECs as follows:

$$\langle \mathcal{B}|\mathcal{O}^{\lambda_k^{\mathrm{PQ}}}|\mathcal{B}\rangle_{\text{1-loop}} = \frac{1}{\beta}\langle \mathcal{B}|\mathcal{O}^{\lambda_k^{\mathrm{PQ}}}|\mathcal{B}\rangle - C_{\mathcal{B}}^k, \tag{59}$$

where $\mathcal{B}$ denotes the external single-b hadron, while β denotes the LECs β_1 and β_3' for B mesons and Λ_b baryon, respectively. Here we use the subtraction scheme defined in Eq. 58 and neglect the analytic terms in Eq. 50 and Eq. 51. The results of one-loop calculations are summarized in Fig. 7 for external B_d and B_s, and in Fig. 8 for Λ_b. In each figure, the black dashed line is the LO contribution, while the blue and red solid curves are the connected and disconnected one-loop contributions, respectively; we use the central values of g_1 and g_3 with the ratios of LECs being unity, $\beta_2/\beta_1 = (-\beta_1' + 2\beta_2')/\beta_3' = 1$. The variations of the axial couplings and of both the axial couplings and the ratios of LECs are represented by the inner dark-shaded and outer light-shaded regions, respectively. It is clear from these figures that the sunset diagrams provide an important part of the disconnected one-loop contributions to the matrix elements, and thus invoke a relatively large uncertainties due to the unknown

[13] In the SU(2) limit, where the mass of strange mesons can be treated on the same order as the chiral symmetry breaking scale, such logarithms vanish and we recover the subtraction scheme used in the context of SU(2) theory [37].

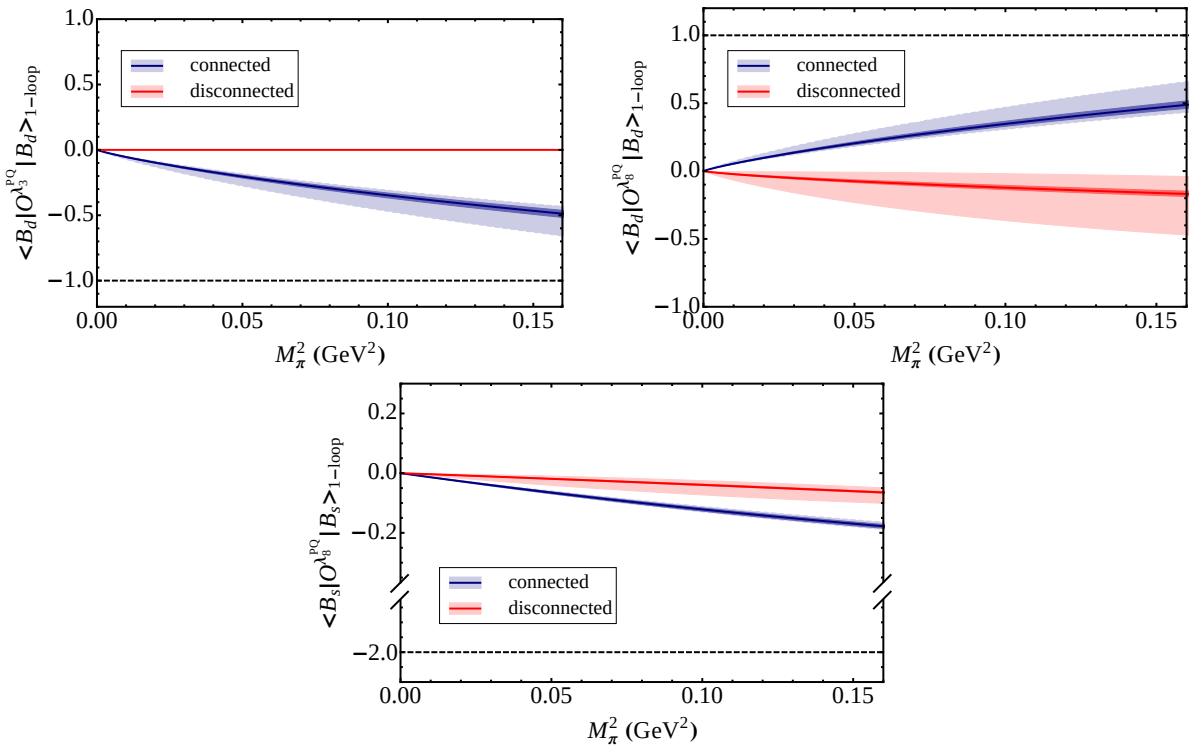

FIG. 7: Infinite-volume one-loop contributions to the matrix elements of $\Delta B = 0$ four-quark operators containing an external B_d for $\lambda_3^{\rm PQ}$ (top-left) and $\lambda_8^{\rm PQ}$ octets (top-right), and B_s for $\lambda_8^{\rm PQ}$ octet (bottom). For references, black dashed lines correspond to the LO contributions. Blue and red colors represent the connected and disconnected one-loop contributions, respectively; solid lines are obtained using $g_1 = 0.449$ and $\beta_2/\beta_1 = 1$, while inner and outer shaded regions are obtained by varying g_1 and both g_1 and $|\beta_2/\beta_1|$ over the range given in the text, respectively.

LECs for B^* mesons and S-type baryons. In addition, the matrix elements containing external B_s have relatively small pion-mass dependence compared to those containing B_d because of the absence of pion loops, where their logarithmic behavior almost fades away.

For idealized values of LECs, namely $\beta_2 = \beta_1$ and $\beta_3' = -\beta_1' + 2\beta_2'$, the disconnected diagrams provide a sizable contribution to the matrix elements for the $\lambda_8^{\rm PQ}$ octet because of large SU(3) breaking effects in the light-quark sector. In the case of the $\lambda_3^{\rm PQ}$ octet, the matrix elements containing B_s and Λ_b do not exist to all orders in the chiral expansion provided isospin symmetry is exact. As seen in Fig. 7, on the other hand, the matrix element containing B_d receives connected one-loop contributions which are exactly opposite to those for the $\lambda_8^{\rm PQ}$ octet, but it receives no disconnected contributions. Since the eye-

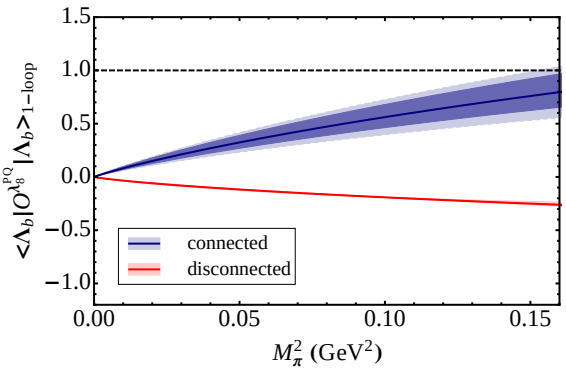

FIG. 8: Infinite-volume one-loop contributions to the matrix elements of $\Delta B = 0$ four-quark operators containing an external Λ_b baryon for $\lambda_8^{\rm PQ}$ octet. For references, black dashed lines correspond to the LO contributions. Blue and red colors represent the connected and disconnected one-loop contributions, respectively; solid lines are obtained using $g_3 = 0.71$ and $(-\beta_1' + 2\beta_2')/\beta_3' = 1$, while inner and outer shaded regions are obtained by varying g_3 and both g_3 and $|(-\beta_1' + 2\beta_2')/\beta_3'|$ over the range given in the text, respectively.

contractions also vanish, one can in principle determine this matrix element very accurately from the calculation of connected diagrams which are accessible by current lattice techniques. Moreover, its precise value will play a crucial role in the investigation of the life-time ratio $\tau(B^+)/\tau(B_d)$ [16].

Now, we explore the finite volume effects in $\Delta B = 0$ matrix elements for external B_d, B_s mesons, and Λ_b baryon. To this end, we consider the change in the finite volume matrix elements relative to the infinite ones normalized by their three-level values,

$$\langle \mathcal{B}|\mathcal{O}^{\lambda_k^{\rm PQ}}|\mathcal{B}\rangle_{\rm FV} = \frac{\langle \mathcal{B}|\mathcal{O}^{\lambda_k^{\rm PQ}}|\mathcal{B}\rangle(L) - \langle \mathcal{B}|\mathcal{O}^{\lambda_k^{\rm PQ}}|\mathcal{B}\rangle(\infty)}{\langle \mathcal{B}|\mathcal{O}^{\lambda_k^{\rm PQ}}|\mathcal{B}\rangle_{\rm tree}}, \tag{60}$$

where $\mathcal{B}$ denotes the external single-b hadron. With a lattice volume fixed by $L = 2.5$ fm we present the results for B_d, B_s in Fig. 9, and for Λ_b in Fig. 10, where the blue and red solid curves are the connected and disconnected one-loop contributions; we use the central values of g_1 and g_3 with the ratios of LECs being unity, $\beta_2/\beta_1 = (-\beta_1' + 2\beta_2')/\beta_3' = 1$. The variations of the axial couplings and of both the axial coupling and the ratios of LECs are represented by the inner dark-shaded and outer light-shaded regions, respectively. In the case of B_d finite volume effects in the connected diagrams for $\lambda_3^{\rm PQ}$ are exactly same with those for the $\lambda_8^{\rm PQ}$ octet, while the effects in the disconnected diagrams vanish. In the cases

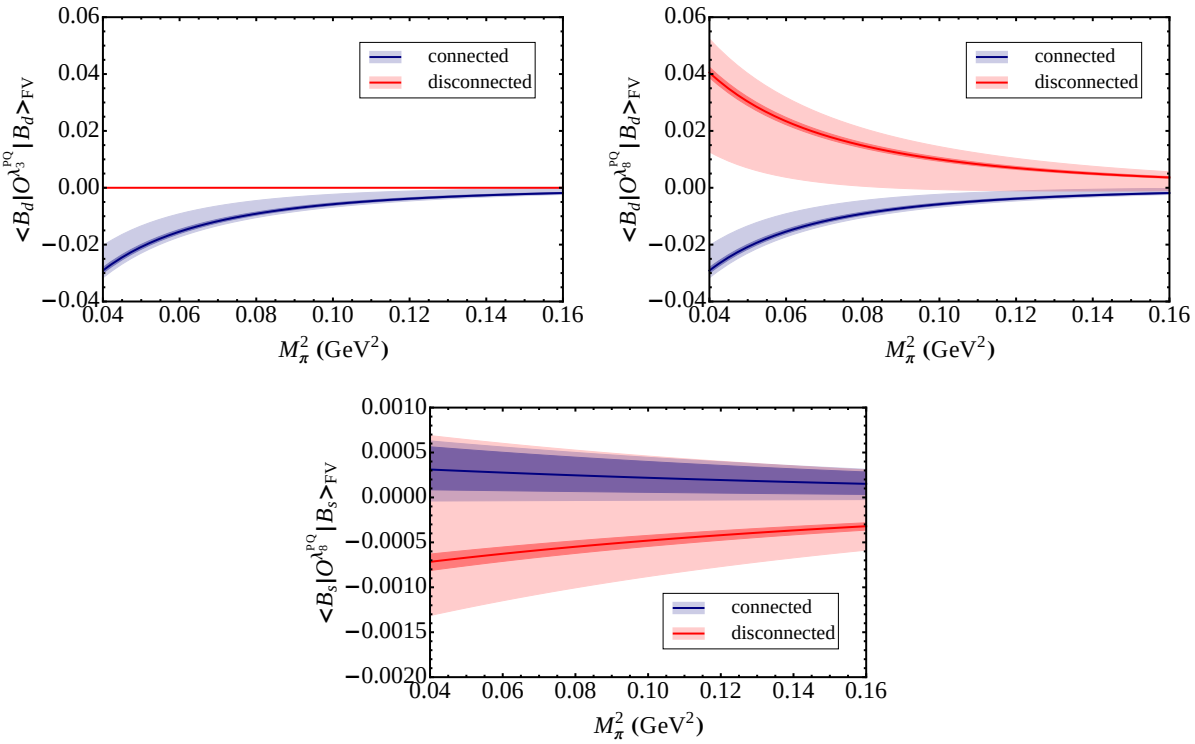

FIG. 9: Finite volume effects in the matrix elements of $\Delta B = 0$ four-quark operators containing external B_d, for $\lambda_3^{\rm PQ}$ (top-left) and $\lambda_8^{\rm PQ}$ octets (top-right), and B_s for $\lambda_8^{\rm PQ}$ octet (bottom) over the range of $m_\pi L$ from 2.5 to 5 in a $L = 2.5$fm lattice. The details are same with those in Fig. 7.

of B_s and Λ_b, the change in Eq. 60 for $\lambda_3^{\rm PQ}$ is ill-defined because the corresponding tree-level matrix elements do not exist. Finite volume effects for B_s are considerably suppressed because pion loops do not contribute to these matrix elements in the QCD limit, while the sizes of finite volume effects for Λ_b are similar to those for B_d. As seen in these figures, the dominant uncertainty in our calculations, especially for the disconnected contributions, arises from the variation of the ratio of unknown LECs.

V. CONCLUSION

We have determined the matrix elements of $\Delta B = 0$ four-quark operators involving single-b hadron external states relevant for the calculation of V_{ub} and lifetimes of single-b hadrons at the next-to-leading order in heavy hadron chiral perturbation theory. We performed these calculations in SU(6|3) partially quenched theories including finite volume effects in the isospin limit, where connected and disconnected contributions are analyzed in a

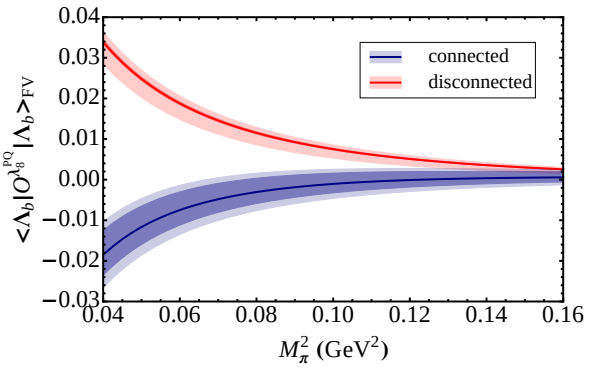

FIG. 10: Finite volume effects in the matrix elements of $\Delta B = 0$ four-quark operators containing an external Λ_b baryon for $\lambda_8^{\rm PQ}$ octet over the range of $m_\pi L$ from 2.5 to 5 in a $L = 2.5$fm lattice. The details are same with those in Fig. 8.

natural manner. At the tree level, the disconnected contributions called the eye-contractions vanish for the octet operators due to the light-flavor symmetry, but they do not for the singlet operator. At the next-to-leading order in chiral expansion for the exemplified cases of external B_d, B_s, and Λ_b, we find that for the $\lambda_8^{\rm PQ}$ octet the disconnected contributions are suppressed but still sizable due to the large light-flavor symmetry breaking. In the case of the $\lambda_3^{\rm PQ}$ octet with an external B_d meson, on the other hand, we find that the matrix elements receive contributions solely from connected diagrams. This result suggests that the precise calculation of these particular matrix elements, which have phenomenological impact on the determination of the lifetime ratio $\tau(B^+)/\tau(B_d)$, is possible using current lattice techniques.

Additionally, our results are necessary to extrapolate the QCD and PQQCD lattice data of these matrix elements from the unphysical light-quark masses used in the finite volume lattice simulations to their physical values. We find that such chiral extrapolations are complicated by more than two unrelated low-energy constants appearing in the leading-order matrix elements in Eqs. 39 and 47. Finite volume effects are at the few-percent level for a lattice volume of $L = 2.5$ fm, and should be taken account into the extrapolations as they become important in high-precision calculations.

Acknowledgments

The author would like to acknowledge William Detmold and C.-J. David Lin for their contributions to the early stage of this work, and for helpful discussions. The author also thanks Brian C. Tiburzi for many fruitful discussions and comments. This work is supported by the U.S. National Science Foundation, under Grant No. PHY12-05778.

---

[1] M. Neubert and C. T. Sachrajda, Nucl.Phys. **B483**, 339 (1997), hep-ph/9603202.

[2] F. Gabbiani, A. I. Onishchenko, and A. A. Petrov, Phys.Rev. **D68**, 114006 (2003), hep-ph/0303235.

[3] Y. Amhis et al. (Heavy Flavor Averaging Group) (2012), 1207.1158.

[4] J. Chay, H. Georgi, and B. Grinstein, Phys.Lett. **B247**, 399 (1990).

[5] I. I. Bigi, N. Uraltsev, and A. Vainshtein, Phys.Lett. **B293**, 430 (1992), hep-ph/9207214.

[6] I. I. Bigi, M. A. Shifman, N. Uraltsev, and A. I. Vainshtein, Phys.Rev.Lett. **71**, 496 (1993), hep-ph/9304225.

[7] A. V. Manohar and M. B. Wise, Phys.Rev. **D49**, 1310 (1994), hep-ph/9308246.

[8] S. Stone (2014), 1406.6497.

[9] M. Di Pierro and C. T. Sachrajda (UKQCD Collaboration), Nucl.Phys. **B534**, 373 (1998), hep-lat/9805028.

[10] D. Becirevic, PoS **HEP2001**, 098 (2001), hep-ph/0110124.

[11] M. Di Pierro, C. T. Sachrajda, and C. Michael (UKQCD collaboration), Phys.Lett. **B468**, 143 (1999), hep-lat/9906031.

[12] M. Baek, J. Lee, C. Liu, and H. Song, Phys.Rev. **D57**, 4091 (1998), hep-ph/9709386.

[13] H.-Y. Cheng and K.-C. Yang, Phys.Rev. **D59**, 014011 (1999), hep-ph/9805222.

[14] C.-S. Huang, C. Liu, and S.-L. Zhu, Phys.Rev. **D61**, 054004 (2000), hep-ph/9906300.

[15] C. Tarantino (2007), hep-ph/0702235.

[16] A. Lenz (2014), 1405.3601.

[17] A. Lenz and U. Nierste (2011), 1102.4274.

[18] M. Neubert, Phys.Rev. **D49**, 3392 (1994), hep-ph/9311325.

[19] M. Neubert, Phys.Rev. **D49**, 4623 (1994), hep-ph/9312311.

[20] I. I. Bigi, M. A. Shifman, N. Uraltsev, and A. Vainshtein, Int.J.Mod.Phys. **A9**, 2467 (1994), hep-ph/9312359.

[21] S. J. Lee, M. Neubert, and G. Paz, Phys.Rev. **D75**, 114005 (2007), hep-ph/0609224.

[22] M. Benzke, S. J. Lee, M. Neubert, and G. Paz, JHEP **1008**, 099 (2010), 1003.5012.

[23] B. Grinstein, Nucl.Phys. **B339**, 253 (1990).

[24] E. Eichten and B. R. Hill, Phys.Lett. **B234**, 511 (1990).

[25] H. Georgi, Phys.Lett. **B240**, 447 (1990).

[26] M. Voloshin, Phys.Lett. **B515**, 74 (2001), hep-ph/0106040.

[27] M. A. Shifman, A. Vainshtein, and V. I. Zakharov, Nucl.Phys. **B147**, 385 (1979).

[28] M. A. Shifman, A. Vainshtein, and V. I. Zakharov, Nucl.Phys. **B147**, 448 (1979).

[29] M. Neubert and T. Becher, Phys.Lett. **B535**, 127 (2002), hep-ph/0105217.

[30] G. Burdman and J. F. Donoghue, Phys.Lett. **B280**, 287 (1992).

[31] M. B. Wise, Phys.Rev. **D45**, 2188 (1992).

[32] T.-M. Yan, H.-Y. Cheng, C.-Y. Cheung, G.-L. Lin, Y. Lin, et al., Phys.Rev. **D46**, 1148 (1992).

[33] P. L. Cho, Phys.Lett. **B285**, 145 (1992), hep-ph/9203225.

[34] P. L. Cho, Nucl.Phys. **B396**, 183 (1993), hep-ph/9208244.

[35] D. Arndt and C. J. D. Lin, Phys. Rev. **D70**, 014503 (2004), hep-lat/0403012.

[36] W. Detmold and C. J. D. Lin, Phys. Rev. **D76**, 014501 (2007), hep-lat/0612028.

[37] W. Detmold, C. J. D. Lin, and S. Meinel, Phys. Rev. **D84**, 094502 (2011), 1108.5594.

[38] C. W. Bernard and M. F. Golterman, Phys.Rev. **D49**, 486 (1994), hep-lat/9306005.

[39] D. Becirevic, S. Fajfer, and J. F. Kamenik, Phys.Lett. **B671**, 66 (2009), 0804.1750.

[40] S. R. Sharpe and Y. Zhang, Phys.Rev. **D53**, 5125 (1996), hep-lat/9510037.

[41] M. J. Savage, Phys.Rev. **D65**, 034014 (2002), hep-ph/0109190.

[42] C. G. Boyd and B. Grinstein, Nucl.Phys. **B442**, 205 (1995), hep-ph/9402340.

[43] B. Grinstein, E. E. Jenkins, A. V. Manohar, M. J. Savage, and M. B. Wise, Nucl.Phys. **B380**, 369 (1992), hep-ph/9204207.

[44] G. Chiladze, Phys.Rev. **D57**, 5586 (1998), hep-ph/9704426.

[45] J.-W. Chen and M. J. Savage, Phys.Rev. **D65**, 094001 (2002), hep-lat/0111050.

[46] B. C. Tiburzi, Phys.Rev. **D71**, 034501 (2005), hep-lat/0410033.

[47] S. R. Sharpe and N. Shoresh, Phys.Rev. **D64**, 114510 (2001), hep-lat/0108003.

[48] S. R. Sharpe and N. Shoresh, Phys.Rev. **D62**, 094503 (2000), hep-lat/0006017.

[49] D. Arndt, S. R. Beane, and M. J. Savage, Nucl.Phys. **A726**, 339 (2003), nucl-th/0304004.

[50] T. Aaltonen et al. (CDF Collaboration), Phys.Rev.Lett. **99**, 202001 (2007), 0706.3868.

[51] M. Golterman and E. Pallante, JHEP **0110**, 037 (2001), hep-lat/0108010.

[52] M. J. Savage and M. B. Wise, Nucl.Phys. **B326**, 15 (1989).

[53] S. R. Sharpe, Phys.Rev. **D46**, 3146 (1992), hep-lat/9205020.

[54] K. Olive et al. (Particle Data Group), Chin.Phys. **C38**, 090001 (2014).

[55] W. Detmold, C.-J. D. Lin, and S. Meinel, Phys.Rev.Lett. **108**, 172003 (2012), 1109.2480.

[56] W. Detmold, C. D. Lin, and S. Meinel, Phys.Rev. **D85**, 114508 (2012), 1203.3378.

[57] B. C. Tiburzi and A. Walker-Loud, Nucl.Phys. **A764**, 274 (2006), hep-lat/0501018.

[58] A. Walker-Loud (2006), hep-lat/0608010.

[59] J. Gasser and H. Leutwyler, Nucl.Phys. **B250**, 465 (1985).

Appendix A: Integrals and sums

The ultra-violet divergences in various loop integrals are regularized by dimensional regularization and have the term

$$\bar{\lambda} = \frac{2}{4-d} - \gamma_E + \log(4\pi) + 1, \tag{A1}$$

where d is the number of space-time dimension. This is a commonly used scheme in χPT calculations [59], which is different from the $\overline{\rm MS}$ scheme by the constant "1" on the right-hand side of the above equation. The requisite subtracted integrals appearing in the one-loop calculations in the framework of PQχPT can all be obtained from the following integrals,

$$\begin{aligned} I(m) &\equiv \mu^{4-d} \int \frac{d^d k}{(2\pi)^d} \frac{1}{k^2 - m^2 + i\epsilon} - \frac{i m^2}{16\pi^2}\bar{\lambda} \\ &= -\frac{i m^2}{16\pi^2} \log\left(\frac{m^2}{\mu^2}\right), \end{aligned} \tag{A2}$$

$$\begin{aligned} F(m,\Delta) &\equiv (g^{\rho\nu} - v^\rho v^\nu) \left[\frac{\mu^{4-d}}{(d-1)} \int \frac{d^d k}{(2\pi)^d} \frac{k_\rho k_\nu}{(k^2 - m^2 + i\epsilon)(v\cdot k - \Delta + i\epsilon)} \right. \\ &\qquad \left. - \frac{i g_{\rho\nu}}{16\pi^2}\bar{\lambda}\left(\frac{2\Delta^2}{3} - m^2\right)\Delta \right] \\ &= \frac{i}{16\pi^2}\left[\log\left(\frac{m^2}{\mu^2}\right)\left(m^2 - \frac{2}{3}\Delta^2\right)\Delta + \left(\frac{10}{9}\Delta^2 - \frac{4}{3}m^2\right)\Delta + \frac{2(\Delta^2 - m^2)}{3} m R\left(\frac{\Delta}{m}\right)\right], \end{aligned} \tag{A3}$$

where μ is the renormalization scale and with

$$R(x) \equiv \sqrt{x^2-1}\log\left(\frac{x-\sqrt{x^2-1+i\epsilon}}{x+\sqrt{x^2-1+i\epsilon}}\right). \tag{A4}$$

To study finite volume effects in the limit $mL \gg 1$, we consider a cubic spatial box of $V = L^3$ with periodic boundary conditions. The three-momenta are quantized as $\vec{k} = (2\pi/L)\,\vec{e}$, where $e_1, e_2, e_3 = -L/2+1, \cdots, L/2$. After subtracting the ultra-violet divergence like as in Eq. A2 and Eq. A3, we instead obtain the sums

$$\begin{aligned}\mathcal{I}(m) &\equiv \frac{1}{L^3}\sum_{\vec{k}}\int\frac{dk_0}{2\pi}\frac{1}{k^2-m^2+i\epsilon} \\ &= I(m) + I_{FV}(m),\end{aligned} \tag{A5}$$

$$\begin{aligned}\mathcal{F}(m,\Delta) &\equiv \frac{(g^{\rho\nu}-v^\rho v^\nu)}{(d-1)}\frac{1}{L^3}\sum_{\vec{k}}\int\frac{dk_0}{2\pi}\frac{k_\rho k_\nu}{(k^2-m^2+i\epsilon)(v\cdot k-\Delta+i\epsilon)} \\ &= F(m,\Delta) + F_{FV}(m,\Delta).\end{aligned} \tag{A6}$$

The finite-volume pieces are given by [35–37]

$$\begin{aligned}I_{FV}(m) &= \frac{-i}{4\pi^2}m\sum_{\vec{n}\neq\vec{0}}\frac{1}{nL}K_1(nmL) \\ &\overset{mL\gg1}{\longrightarrow} \frac{-i}{4\pi^2}\sum_{\vec{n}\neq\vec{0}}\sqrt{\frac{m\pi}{2nL}}\left(\frac{1}{nL}\right)e^{-nmL}\times\left\{1+\frac{3}{8nmL}-\frac{15}{128(nmL)^2}+\mathcal{O}\left(\left[\frac{1}{nmL}\right]^3\right)\right\}, \\ F_{FV}(m,\Delta) &= \frac{i}{12\pi^2}\sum_{\vec{n}\neq\vec{0}}\frac{1}{nL}\int_0^\infty d|\vec{k}|\frac{|\vec{k}|\sin(n|\vec{k}|L)}{\sqrt{|\vec{k}|^2+m^2}+\Delta}\left(\Delta+\frac{m^2}{\sqrt{|\vec{k}|^2+m^2}}\right), \\ &\overset{mL\gg1}{\longrightarrow} \frac{i}{24\pi}m^2\sum_{\vec{n}\neq\vec{0}}\frac{e^{-nmL}}{nL}\mathcal{A}\end{aligned} \tag{A7}$$

where $\vec{n} = (n_1, n_2, n_3)$ with $n_i \in \mathbb{Z}$, $n \equiv |\vec{n}|$, and

$$\begin{aligned}\mathcal{A} &= e^{(z^2)}[1-\mathrm{Erf}(z)] + \left(\frac{1}{nmL}\right)\left[\frac{1}{\sqrt{\pi}}\left(\frac{9z}{4}-\frac{z^3}{2}\right)+\left(\frac{z^4}{2}-2z^2\right)e^{(z^2)}[1-\mathrm{Erf}(z)]\right] \\ &\quad+\left(\frac{1}{nmL}\right)^2\left[\frac{1}{\sqrt{\pi}}\left(\frac{39z}{64}-\frac{11z^3}{32}+\frac{9z^5}{16}-\frac{z^7}{8}\right)-\left(\frac{z^6}{2}-\frac{z^8}{8}\right)e^{(z^2)}[1-\mathrm{Erf}(z)]\right]+\mathcal{O}\left(\left[\frac{1}{nmL}\right]^3\right),\end{aligned}$$

with

$$z \equiv \left(\frac{\Delta}{m}\right)\sqrt{\frac{nmL}{2}}.$$

The functions appearing in the one-loop results are

$$\mathcal{H}(m,\Delta) \equiv \frac{\partial \mathcal{F}(m,\Delta)}{\partial \Delta}, \tag{A8}$$

and

$$\begin{aligned}\tilde{\mathcal{H}}(M_{a,b},\Delta) \;=\; & \delta_{a,b}\{A_{a,b}\mathcal{H}(M_{a,b},\Delta)+(1-A_{a,b})\mathcal{H}(M_X,\Delta)+C_{a,b}\mathcal{H}_{\eta'}(M_{a,b},\Delta)\} \\ & +(1-\delta_{a,b})\{D^{(a)}_{a,b}\mathcal{H}(M_{a,a},\Delta)+D^{(b)}_{a,b}\mathcal{H}(M_{b,b},\Delta)+D^{(X)}_{a,b}\mathcal{H}(M_X,\Delta)\},\end{aligned} \tag{A9}$$

where the function $\mathcal{H}_{\eta'}$ from the integral of hairpin diagrams is

$$\mathcal{H}_{\eta'}(m,\Delta) \equiv \frac{\partial \mathcal{H}(m,\Delta)}{\partial m^2}. \tag{A10}$$

The coefficients in the function $\tilde{\mathcal{H}}$ are defined by

$$\begin{aligned}
A_{u,u} &= \frac{2\left(\delta_{VS}^2 - M_\pi^2 + M_X^2\right)\delta_{VS}^2}{(M_\pi^2 - M_X^2)^2} + \frac{3}{2}, \quad A_{s,s} = \frac{3\left(8\delta_{VSs}^4 + \left(2\delta_{VS}^2 - M_\pi^2 + M_{s,s}^2\right)^2\right)}{\left(2\delta_{VS}^2 + 4\delta_{VSs}^2 - M_\pi^2 + M_{s,s}^2\right)^2}, \\
C_{u,u} &= 3\delta_{VS}^2 - \frac{2\delta_{VS}^4}{M_\pi^2 - M_X^2}, \quad C_{s,s} = \frac{6\delta_{VSs}^2\left(2\delta_{VS}^2 - M_\pi^2 + M_{s,s}^2\right)}{2\delta_{VS}^2 + 4\delta_{VSs}^2 - M_\pi^2 + M_{s,s}^2}, \\
D_{u,s}^{(u)} &= \frac{2\delta_{VS}^2\left(M_\pi^2 - M_{s,s}^2 + 2\delta_{VSs}^2\right)}{(M_\pi^2 - M_{s,s}^2)(M_\pi^2 - M_X^2)}, \quad D_{u,s}^{(s)} = \frac{2\delta_{VSs}^2\left(M_\pi^2 - M_{s,s}^2 - 2\delta_{VS}^2\right)}{(M_\pi^2 - M_{s,s}^2)(M_{s,s}^2 - M_X^2)}, \\
D_{u,s}^{(X)} &= \frac{(M_\pi^2 - M_X^2 - 2\delta_{VS}^2)(M_{s,s}^2 - M_X^2 - 2\delta_{VSs}^2)}{(M_\pi^2 - M_X^2)(M_{s,s}^2 - M_X^2)},
\end{aligned} \tag{A11}$$

where $M_{a,b}^2 = B_0(m_a + m_b)$, $\delta_{VS}^2 = M_{u,u}^2 - M_{u,j}^2$, $\delta_{VSs}^2 = M_{s,s}^2 - M_{s,r}^2$, $M_\pi = M_{u,u}$, and $M_X^2 = \frac{1}{3}\left(M_{u,u}^2 + 2M_{s,s}^2 - 2\delta_{VS}^2 - 4\delta_{VSs}^2\right)$. Notice that we take the isospin limit as in Eq. 20. In the QCD limit (setting valence and sea quark masses to be identical), we have

$$\begin{aligned}
&A_{u,u}^{QCD} = \frac{3}{2}, \quad A_{s,s}^{QCD} = 3, \quad C_{u,u}^{QCD} = 0, \quad C_{s,s}^{QCD} = 0, \\
&D_{u,s}^{(u)QCD} = 0, \quad D_{u,s}^{(s)QCD} = 0, \quad D_{u,s}^{(X)QCD} = 1.
\end{aligned} \tag{A12}$$

Appendix B: coefficients for chiral one-loop contributions in B-meson

In this appendix, we present the coefficients in Eq. 53 and Eq. 54 corresponding to the tadpole- and sunset-type diagrams. These coefficients are summarized in Table III and Table IV.

TABLE III: Coefficients $x^{B,k}_{\phi_{ab}}$ and $\bar{x}^{B,k}_{\phi_{ab}}$ in Eq. 53 in the isospin limit. In the case of B_d, the coefficients for $k = 0, 8$ and for $k = 3$ are identical and opposite to those of B_u, respectively. The coefficients for B_s with $k = 3$ are all zeros.

		$x^{B,k}_{\phi}$				$\bar{x}^{B,k}_{\phi}$			
		uj	ur	sj	sr	uj	ur	sj	sr
$k=0$	B_u	-2	-1	0	0	2	1	0	0
	B_s	0	0	-2	-1	0	0	2	1
$k=3$	B_u	-2	-1	0	0	0	0	0	0
$k=8$	B_u	-2	-1	0	0	2	-2	0	0
	B_s	0	0	4	2	0	0	2	-2

TABLE IV: Coefficients $\bar{y}^{B,k}_{\phi_{ab}}$ and $\tilde{y}^{B,k}_{\phi_{aa}\phi'_{bb}}$ in Eq. 54 in the isospin limit. In the case of B_d, the coefficients for $k = 0, 8$ and for $k = 3$ are identical and opposite to those of B_u, respectively. The coefficients for B_s with $k = 3$ are all zeros.

		$\bar{y}^{B,k}_{\phi}$				$\tilde{y}^{B,k}_{\phi\phi'}$		
		uj	ur	sj	sr	$\eta_u\eta_u$	$\eta_u\eta_s$	$\eta_s\eta_s$
$k=0$	B_u	6	3	0	0	1	0	0
	B_s	0	0	6	3	0	0	1
$k=3$	B_u	0	0	0	0	1	0	0
$k=8$	B_u	6	-6	0	0	1	0	0
	B_s	0	0	6	-6	0	0	-2

Appendix C: Coefficients for chiral one-loop contributions in B-baryon

In this appendix, we present the coefficients in Eq. 55, Eq. 56, and Eq. 58 corresponding to the self-energy, tadpole, and sunset one-loop diagrams. These coefficients are summarized in Table V, Table VI, Table VII, Table VIII, and Table IX.

TABLE V: Coefficients $w^{T(S)}_{\phi_{ab}}$, $w'^{S}_{\phi_{ab}}$, $\tilde{w}^{T(S)}_{\phi_{aa}\phi'_{bb}}$, and $\tilde{w}'^{S}_{\phi_{aa}\phi'_{bb}}$ in Eq. 55 in the isospin limit. Σ, Ξ, and Ξ' baryons with different 3-components of the isospin have the same coefficients because of the isospin symmetry. ϕ_{us} and ϕ_{su} are distinguished by the appearance of their mass parameters $\delta^{(B)}_{us}$ and $-\delta^{(B)}_{us}$ in the propagator of internal baryons.

	w_ϕ								$w_{\phi\phi'}$		
	uu	us	su	ss	uj	ur	sj	sr	$\eta_u\eta_u$	$\eta_u\eta_s$	$\eta_s\eta_s$
Λ_b	3	0	0	0	6	3	0	0	0	0	0
Ξ_b	0	$\frac{3}{2}$	$\frac{3}{2}$	0	3	$\frac{3}{2}$	3	$\frac{3}{2}$	$\frac{1}{2}$	-1	$\frac{1}{2}$
Σ	1	0	0	0	2	1	0	0	$\frac{2}{3}$	0	0
Ξ'	0	$\frac{1}{2}$	$\frac{1}{2}$	0	1	$\frac{1}{2}$	1	$\frac{1}{2}$	$\frac{1}{6}$	$\frac{1}{3}$	$\frac{1}{6}$
Ω	0	0	0	1	0	0	2	1	0	0	$\frac{2}{3}$
	w'_ϕ								$w'_{\phi\phi'}$		
Σ	-1	0	0	0	2	1	0	0	0	0	0
Ξ'	0	$-\frac{1}{2}$	$-\frac{1}{2}$	0	1	$\frac{1}{2}$	1	$\frac{1}{2}$	$\frac{1}{6}$	$-\frac{1}{3}$	$\frac{1}{6}$
Ω	0	0	0	-1	0	0	2	1	0	0	0

TABLE VI: Coefficients $x_{\phi_{ab}}^{T(S),k}$ and $\bar{x}_{\phi_{ab}}^{T(S),k}$ in Eq. 56 in the isospin limit. For $k = 0, 8$, we find $x_\phi^{\Lambda_b} = x_\phi^{\Sigma_b}$, $\bar{x}_\phi^{\Lambda_b} = \bar{x}_\phi^{\Sigma_b}$, $x_\phi^{\Xi_b} = x_\phi^{\Xi'_b}$, and $\bar{x}_\phi^{\Xi_b} = \bar{x}_\phi^{\Xi'_b}$, where Σ, Ξ, and Ξ' baryons with different 3-components of the isospin have the same coefficients because of isospin symmetry. For $k = 3$, we find $x_\phi^{\Sigma_b^-} = -x_\phi^{\Sigma_b^+}$ and $x_\phi^{\Xi_b^{-\frac{1}{2}}} = x_\phi^{\Xi_b^{\prime -\frac{1}{2}}} = -x_\phi^{\Xi_b^{+\frac{1}{2}}} = -x_\phi^{\Xi_b^{\prime +\frac{1}{2}}}$, while $x_\phi^{\Lambda_b} = x_\phi^{\Sigma_b^0} = x_\phi^{\Omega_b} = 0$ for possible Goldstone mesons. Coefficients $\bar{x}$ are all zeros for $k = 3$.

		$x_\phi^{T(S),k}$				$\bar{x}_\phi^{T(S),k}$			
		uj	ur	sj	sr	uj	ur	sj	sr
$k=0$	Λ_b	-2	-1	0	0	2	1	0	0
	Ξ	-1	$-\frac{1}{2}$	-1	$-\frac{1}{2}$	1	$\frac{1}{2}$	1	$\frac{1}{2}$
	Ω	0	0	-2	-1	0	0	2	1
$k=3$	$\Xi^{+\frac{1}{2}}$	-1	$-\frac{1}{2}$	0	0	0	0	0	0
	Σ^+	-2	-1	0	0	0	0	0	0
$k=8$	Λ_b	-2	-1	0	0	2	-2	0	0
	Ξ	-1	$-\frac{1}{2}$	2	1	1	-1	1	-1
	Ω	0	0	4	2	0	0	2	-2

TABLE VII: Coefficients $y^{T,k}_{\phi_{ab}}$, $\bar{y}^{T,k}_{\phi_{ab}}$ and $\tilde{y}^{T,k}_{\phi_{aa}\phi'_{bb}}$ in Eq. 58 in the isospin limit. The unbarred coefficients of $\Xi_b^{-\frac{1}{2}}$ are identical and opposite to those of $\Xi_b^{\frac{1}{2}}$ for $k = 0, 8$ and $k = 3$, respectively; the unbarred coefficients of Λ_b are all zeros for $k = 3$. The barred coefficients of $\Xi_b^{-\frac{1}{2}}$ are identical to those of $\Xi_b^{\frac{1}{2}}$ for $k = 0, 8$, while the barred coefficients are all zeros for $k = 3$. ϕ_{us} and ϕ_{su} are distinguished by the appearance of their mass parameters δ_{us} and $-\delta_{us}$ in the propagator of internal baryons.

		$y^{T,k}_{\phi}$								$\tilde{y}^{T,k}_{\phi\phi'}$		
		uu	us	su	ss	uj	ur	sj	sr	$\eta_u\eta_u$	$\eta_u\eta_s$	$\eta_s\eta_s$
$k=0$	Λ_b	1	0	0	0	1	$\frac{1}{2}$	0	0	$\frac{2}{3}$	0	0
	$\Xi_b^{+\frac{1}{2}}$	0	$\frac{1}{2}$	$\frac{1}{2}$	0	$\frac{1}{2}$	$\frac{1}{4}$	$\frac{1}{2}$	$\frac{1}{4}$	$\frac{1}{6}$	$\frac{1}{3}$	$\frac{1}{6}$
$k=3$	$\Xi_b^{+\frac{1}{2}}$	0	0	$\frac{1}{2}$	0	0	0	$\frac{1}{2}$	$\frac{1}{4}$	$\frac{1}{12}$	$\frac{1}{6}$	$\frac{1}{12}$
$k=8$	Λ_b	1	0	0	0	1	$\frac{1}{2}$	0	0	$\frac{2}{3}$	0	0
	$\Xi_b^{+\frac{1}{2}}$	0	-1	$\frac{1}{2}$	0	-1	$-\frac{1}{2}$	$\frac{1}{2}$	$\frac{1}{4}$	$-\frac{1}{12}$	$-\frac{1}{6}$	$-\frac{1}{12}$
		$\bar{y}^{T,k}_{\phi}$										
$k=0$	Λ_b	0	0	0	0	1	$\frac{1}{2}$	0	0			
	$\Xi_b^{+\frac{1}{2}}$	0	0	0	0	$\frac{1}{2}$	$\frac{1}{4}$	$\frac{1}{2}$	$\frac{1}{4}$			
$k=8$	Λ_b	0	0	0	0	1	-1	0	0			
	$\Xi_b^{+\frac{1}{2}}$	0	0	0	0	$\frac{1}{2}$	$-\frac{1}{2}$	$\frac{1}{2}$	$-\frac{1}{2}$			

TABLE VIII: Coefficients $y^{S,k}_{\phi_{ab}}$, $\bar{y}^{S,k}_{\phi_{ab}}$, and $\tilde{y}^{S,k}_{\phi_{aa}\phi'_{bb}}$ in Eq. 58 in the isospin limit. The unbarred coefficients of Σ_b^-, $\Xi_b^{\prime -}$ are indentical and opposite to those of Σ_b^+, $\Xi_b^{\prime +}$ for $k = 0, 8$ and $k = 3$, respectively; the unbarred coefficients of Σ_b^0 and Ω_b are all zeros for $k = 3$. In the case of barred coefficients, Σ and Ξ' with different 3-componets of the isospin have the same coefficients with those for $k = 0, 8$, while the barred coefficients are all zeros for $k = 3$. ϕ_{us} and ϕ_{su} are distinguished by the appearance of their mass parameters δ_{us} and $-\delta_{us}$ in the propagator of internal baryons.

		$y^{S,k}_{\phi}$								$\tilde{y}^{S,k}_{\phi\phi'}$		
		uu	us	su	ss	uj	ur	sj	sr	$\eta_u\eta_u$	$\eta_u\eta_s$	$\eta_s\eta_s$
$k=0$	Σ_b^0	1	0	0	0	1	$\frac{1}{2}$	0	0	$\frac{2}{3}$	0	0
	Σ_b^+	1	0	0	0	1	$\frac{1}{2}$	0	0	0	0	0
	$\Xi_b^{\prime +\frac{1}{2}}$	0	$\frac{1}{2}$	$\frac{1}{2}$	0	$\frac{1}{2}$	$\frac{1}{4}$	$\frac{1}{2}$	$\frac{1}{4}$	$\frac{1}{6}$	$\frac{1}{3}$	$\frac{1}{6}$
	Ω_b	0	0	0	1	0	0	1	$\frac{1}{2}$	0	0	0
$k=3$	Σ_b^+	1	0	0	0	1	$\frac{1}{2}$	0	0	0	0	0
	$\Xi_b^{\prime +\frac{1}{2}}$	0	0	$\frac{1}{2}$	0	0	0	$\frac{1}{2}$	$\frac{1}{4}$	$\frac{1}{12}$	$\frac{1}{6}$	$\frac{1}{12}$
$k=8$	Σ_b^0	1	0	0	0	1	$\frac{1}{2}$	0	0	$\frac{2}{3}$	0	0
	Σ_b^+	1	0	0	0	1	$\frac{1}{2}$	0	0	0	0	0
	$\Xi_b^{\prime +\frac{1}{2}}$	0	-1	$\frac{1}{2}$	0	-1	$-\frac{1}{2}$	$\frac{1}{2}$	$\frac{1}{4}$	$-\frac{1}{12}$	$-\frac{1}{6}$	$-\frac{1}{12}$
	Ω_b	0	0	0	-2	0	0	-2	-1	0	0	0
		$\bar{y}^{S,k}_{\phi}$										
$k=0$	Σ_b	0	0	0	0	1	$\frac{1}{2}$	0	0			
	Ξ'_b	0	0	0	0	$\frac{1}{2}$	$\frac{1}{4}$	$\frac{1}{2}$	$\frac{1}{4}$			
	Ω_b	0	0	0	0	0	0	1	$\frac{1}{2}$			
$k=8$	Σ_b	0	0	0	0	1	-1	0	0			
	Ξ'_b	0	0	0	0	$\frac{1}{2}$	$-\frac{1}{2}$	$\frac{1}{2}$	$-\frac{1}{2}$			
	Ω_b	0	0	0	0	0	0	1	-1			

TABLE IX: Coefficients $y'^{S,k}_{\phi_{ab}}$, $\bar{y}'^{S,k}_{\phi_{ab}}$, and $\tilde{y}'^{S,k}_{\phi_{aa}\phi'_{bb}}$ in Eq. 58 in the isospin limit. The unbarred coefficients of Σ_b^-, $\Xi_b'^-$ are indentical and opposite to those of Σ_b^+, $\Xi_b'^+$ for $k = 0, 8$ and $k = 3$, respectively; the unbarred coefficients of Σ_b^0 and Ω_b are all zeros for $k = 3$. In the case of barred coefficients, Σ and Ξ' with different 3-componets of the isospin have the same coefficients with those for $k = 0, 8$, while the barred coefficients are all zeros for $k = 3$. ϕ_{us} and ϕ_{su} are distinguished by the appearance of their mass parameters δ_{us} and $-\delta_{us}$ in the propagator of internal baryons.

		$y'^{S,k}_{\phi}$								$\tilde{y}'^{S,k}_{\phi\phi'}$		
		uu	us	su	ss	uj	ur	sj	sr	$\eta_u\eta_u$	$\eta_u\eta_s$	$\eta_s\eta_s$
$k=0$	Σ_b^0	1	0	0	0	-1	$-\frac{1}{2}$	0	0	$-\frac{2}{3}$	0	0
	Σ_b^+	1	0	0	0	-1	$-\frac{1}{2}$	0	0	0	0	0
	$\Xi_b'^{+\frac{1}{2}}$	0	$\frac{1}{2}$	$\frac{1}{2}$	0	$-\frac{1}{2}$	$-\frac{1}{4}$	$-\frac{1}{2}$	$-\frac{1}{4}$	$-\frac{1}{6}$	$-\frac{1}{3}$	$-\frac{1}{6}$
	Ω_b	0	0	0	1	0	0	-1	$-\frac{1}{2}$	0	0	0
$k=3$	Σ_b^+	1	0	0	0	-1	$-\frac{1}{2}$	0	0	0	0	0
	$\Xi_b'^{+\frac{1}{2}}$	0	0	$\frac{1}{2}$	0	0	0	$-\frac{1}{2}$	$-\frac{1}{4}$	$-\frac{1}{12}$	$-\frac{1}{6}$	$-\frac{1}{12}$
$k=8$	Σ_b^0	1	0	0	0	-1	$-\frac{1}{2}$	0	0	$-\frac{2}{3}$	0	0
	Σ_b^+	1	0	0	0	-1	$-\frac{1}{2}$	0	0	0	0	0
	$\Xi_b'^{+\frac{1}{2}}$	0	-1	$\frac{1}{2}$	0	1	$\frac{1}{2}$	$-\frac{1}{2}$	$-\frac{1}{4}$	$\frac{1}{12}$	$\frac{1}{6}$	$\frac{1}{12}$
	Ω_b	0	0	0	-2	0	0	2	1	0	0	0
		$\bar{y}'^{S,k}_{\phi}$										
$k=0$	Σ_b	0	0	0	0	-1	$-\frac{1}{2}$	0	0			
	Ξ_b'	0	0	0	0	$-\frac{1}{2}$	$-\frac{1}{4}$	$-\frac{1}{2}$	$-\frac{1}{4}$			
	Ω_b	0	0	0	0	0	0	-1	$-\frac{1}{2}$			
$k=8$	Σ_b	0	0	0	0	-1	1	0	0			
	Ξ_b'	0	0	0	0	$-\frac{1}{2}$	$\frac{1}{2}$	$-\frac{1}{2}$	$\frac{1}{2}$			
	Ω_b	0	0	0	0	0	0	-1	1			